Mechanisms in the refining zone for development of physical properties of TMP fibres in a low-consistency refiner

Pressure measurements in the refining zone

Oddbjørn Eriksen

2005

Mechanisms in the refining zone for development of physical properties of TMP fibres in a low-consistency refiner

Pressure measurements in the refining zone

Oddbjørn Eriksen

Report no. 114, 2005

Cluster: Mechanical Pulp
Distribution restricted to: Eka Chemicals, Holmen Paper, Norske Skog, Stora Enso, Södra Cell, Ola Johansson, J&L Fiber Services Inc.

a report from STFI-Packforsk

Acknowledgements

This study has been performed as a part of the project LC refining mechanisms within the cluster research program of Mechanical pulp 2003 – 2005. The industrial members of this cluster through the companies Eka Chemicals, Holmen Paper, Norske Skog, Stora Enso and Södra Cell are gratefully acknowledged.

A special recognition is given to Ola Johansson, Technical Director in J&L Fiber Services Inc. for providing the fibre-optic sensors as well as the refiner plates used in the trials at the EuroFEX pilot plant facilities. Mr. Johansson is also gratefully acknowledged for his participation in the trials and as always showing great interest in the scientific work.

The financial contribution from STEM is also gratefully acknowledged.

Table of contents

1 Summary

This technical report shows results from the second of two experimental trials using fibre-optic pressure sensors in the Beloit double disc refiner at the STFI-Packforsk EuroFEX laboratory in Stockholm. The trials were conducted at low-consistency conditions during refining of different types of pulp. Both bleached and unbleached softwood Kraft pulps as well as high-freeness mechanical pulps were used. The first attempt to measure high-frequency pressure pulsations in the refining zone of the 600 mm pilot refiner was performed in the fall 2004. The follow-up trial was conducted in the spring 2005 using a slightly different sensor design. The latest attempt was followed up with an extensive investigation of the sensor performance in the Material Test System (MTS) Laboratory at STFI-Packforsk as well.

The first attempt to measure the pressure pulses in the refining zone gave no clear conclusions because of a few uncertainties associated with the sensors and the measurement system. However, the dynamic response of the sensors seemed not to be disturbed since the frequency analysis of the recordings evidently contained process inherent information. One of the former uncertainties was connected to interference from the electrical grounding, which created offset adjustments of the output signal from the amplifier. This was solved before the second trial. The sinusoidal interferometric signal from the sensors created another uncertainty regarding the determination of the high pressure pulses. Thus, a slightly different sensor design was established before the last trial. This resulted in improved readability, but the resolution of the measured signal was poorer than before. The sacrifice of the resolution in lieu of readability was a drawback in the case of determining the absolute pressure accurately.

The tests performed in the MTS laboratory clearly showed that the sensors responded ideal to pure hydraulic loads. The dynamic response of the sensor was very good as well. The evaluation of the responses while a wet fibre pad was laid on the sensor surface strongly indicates that the fibre network supports parts of the applied load. The latter occurs as a result of a drier fibre network because the water is squeezed out. How relevant this observation is according to the conditions in the plate gap is not assessed more profoundly. Another result from the laboratory tests strongly recommends that the location of the sensor surface determined by the depth below the plate surface should not be more than a few micrometers. A third observation from these tests is interpreted as leakage flow associated to suction forces back and forth to a fibre mat under varying load. The sensor design with an open cavity between the transducer and sensor tubes is assumed creating this undesirable effect. However, the existence of these forces and the corresponding leakage flows are not verified.

The present study has showed that FFT analysis gives information of periodical occurrences in the recordings. Thus, it is possible to extract process inherent properties by the use of frequency analysis of the recordings. The local bar crossing frequency associated to the radial location of the sensors dominated the frequency spectra. This signifies that the sensors measure process inherent properties. Also the sensors ability to reproduce high-frequency pressure fluctuations is evident. In addition, variations in the

local bar crossing frequency have been observed. The latter signifies that the rotational speed of the refiner was slightly different at different runs. However, no systematic changes are found due to different edge loads, flow rates or other operational conditions.

Some results show high pressure spikes that occurred periodically at a rate corresponding to the bar and groove pattern of the plates of the rotating disc. The pressure pulses revealed pressures above 2 MPa. However, the activity at this pressure level occurred infrequently. This indicates that the gap area between the surface of the pressure sensor and the rotor bars was filled with compressed fibres or larger agglomerates of fibre bundles only on rare occasions. The present trial did not enhance the interpretations of the previous trial, which indicated pressure peaks up to 7 MPa. The number of high pressure peaks seemed to be fewer than in the previous trial as well. The explanation of this difference may be that the sensors were slightly different or that the running conditions of the refiner were different. The latter is not likely the reason despite the trials were run at different times. No major differences were introduced in the second trial. Another explanation may be associated to the fact that the latter sensors had poorer resolution, while the readability was improved compared to the previously used sensors. However, it can not be excluded that the location of the sensors in the plate i.e. the depth from the plate surface to the sensor surface might have created differences. A weakness with the trials was that the positioning of the sensors was not exactly determined. Likely, it is necessary to determine the position down to an uncertainty of a few micrometers in the future.

One of the most remarkable results obtained from the last pressure sensor trial was that pressure drops below an evident average pressure level were frequently observed. Mainly, all of the recordings showed such pressure course that occurred frequently at a rate corresponding to the passage of the bar and groove pattern of the rotating disc. The results strongly indicate that negative pressures (below atmospheric conditions) often appeared as well. The pressure drop is interpreted to be the sliding friction loss caused by the contact between the fibre mat in the small plate gap and the bar surfaces of the refiner plates. The friction probably introduced strain in the fibre pad under sealed conditions, which in turn created vacuum-like conditions. However, a velocity change of the pulp suspension through the plate gap might as well give a pressure drop. The latter may be interpreted that the pulp suspension are flowing radial outwards in the grooves influenced by a relative slow speed. When the pulp suspension is dragged into the gap between the opposite bars of the stator and rotor discs, the pulp suspension increases the velocity to the speed of the rotor disc as well as the flow direction is changed to a tangential direction. Thus, both the sliding friction and the increased velocity might give a pressure drop. It is too early to conclude on which of these effects or a combination of these effects play the crucial role of the observed pressure drop.

The initial pressure increase that appeared before the pressure drop was smaller than expected. The pressure rise was probably caused by the squeezing of the fibre mat between the bars on the rotor and stator discs. However, another important concern is associated to how well the pressure is measured in all positions of the rotor bar movement. The location of the sensor was in the centre of a stator bar. If it can be assumed that the pressure is largest at the leading edge of the rotor bar, it can be questioned how well the pressure is measured from the current location of the sensor.

The pressure drop was often followed by very high pressure pulses of short duration. These rapid pressure spikes are interpreted as shock waves generated by implosions of vapour bubbles, which in turn are generated by the observed under-pressures. The generation of shock waves strongly indicates that cavitation effects are present in the low consistency refiner. No similar results are ever reported although it was not unexpected since wear caused by cavitation is commonly experienced.

Some strange pressure readings were also observed when water was pumped through the refiner. The pulses seemed to be very rapid spikes of extremely short duration. This occurred only when the bar intersection area was present. The pressure readings associated with the groove passages were indeed very smooth. The reason why these were visible may be found in the sensor location or in the design of the transducer itself. Intuitively, it is possible that the sensor head was moving back and forth in the tube. This movement may have caused the apparent pressure readings.

It was not intended to determine the absolute pressures to a definite accurate level in this phase of the experimental work. In this state of the work it was important to investigate the performance of the pressure sensors and derive whether the sensors are appropriate for this purpose. The objective was to verify the measurements and contribute to develop a final version of the sensor that gives reproducible recordings. A modified sensor design is suggested to further investigate the reliability of the sensors.

The sensor design is proposed changed based on the odd observation during pumping of water through the refiner along with the observation associated to leakage flows in the transducer tube. The proposal aims at fill the cavity between the sensor and the transducer tube with silicone. This will probably prevent any movements of the sensor head if such movements have taken place. The new design will also prevent any leakage flow of water in and out of the cavity surrounding the sensor head. The existence of these forces and the corresponding leakage flows are not verified. Thus, a modified sensor design is desirable to exclude any uncertainties connected to the sensors and the measurements.

2 Introduction

This technical report has the main focus on the results obtained from the second of two experimental trials using novel fibre-optic pressure sensors in the Beloit double disc refiner at the STFI-Packforsk EuroFEX laboratory in Stockholm. The trials were conducted at low-consistency conditions. The first attempt to measure high-frequency pressure pulsations in the refining zone of the 600 mm pilot refiner was performed in the fall 2004. The follow-up trial was conducted in the spring 2005 using a slightly different sensor design. The new sensor design was based on experience from the previous trial. The last attempt was followed up with an extensive investigation of the sensor performance in the Material Test System (MTS) Laboratory at STFI-Packforsk.

The small-size fibre-optic pressure sensors were designed and manufactured by Luna Innovations Inc., VA, USA. The technology, fitted for refining zone pressure measurements, has been made on commissions from J&L Fibre Services Inc., WI, USA. Technical director Ola Johansson at J&L Fibre Services has participated in the project by providing sensors and refiner plates. The refining zone pressure measurements have been a part of two projects connected to two different research clusters at STFI-Packforsk. The co-operation has accomplished through projects in the Mechanical pulp research cluster and Advanced fibre management cluster programs respectively.

The initial objective of this study was to investigate the performance of the fibre-optic sensors in order to find coherences between the pressures and the operational conditions as well as the pulp properties. However, the complexity of the measurements and the comprehensive amount of data made it necessary to restrict the scope of work. In this state of the work it was important to investigate the performance of the pressure sensors and derive whether the sensors are appropriate for this purpose. The objective was to verify the measurements and contribute to develop a final version of the sensor that gives reproducible recordings.

3 Background

A summary of the reported knowledge of the refining of mechanical pulps in low-consistency refiners is written as a part of the LC refining mechanisms project (Hammar (2004)). Furthermore, a literature survey of measurements in the refining zone of low-consistency refiners is written as well (Hammar and Eriksen (2005)).

The results from the first trial of the on-going project using fibre-optic pressure sensors strongly indicated that the pressure pulses could be very high. It is assumed that the pressure spikes appear from the squeezing of pulp fibres between the bars on the rotor plate and the sensor surface located close to the surface of a bar in the stator plate. Interpretations of the measurements indicated that the pressure spikes could be very high. Pressure pulses of 7 MPa (70 bar) were observed during refining of chemical pulps, while the results pointed towards pressures above 3 MPa (30 bar) when mechanical pulps were treated. Examples of these results are shown in Appendix A as Figures A1 and A4. However, the majority of the pressure pulses seemed to be below 500 kPa (5 bar) regardless of the pulp type. The results suggest that only a few rotor bars are actively involved in high compression of the pulp fibres (Figure A5). Thus, the development of the fibre quality through the refining zone is probably dominated by other mechanisms than the compression of wood fibres. The hypothesis is that the shear forces appearing from less harsh contact between the fibres and the bar surfaces of the plates as well as inter-fibre interactions play an essential role in the refining process. This explanation seems to be valid at least at the radial positions where the pressure sensors were located. However, results obtained from an adjoining research activity within the same project show measurements of vibrations in the refiner housing, which strongly suggests that the main refining action occurs in the outer part of the refining zone (Eriksen (2005)).

Additional results obtained from the first trial indicated that the pressure frequently decreased below the casing pressure. The pressure seemed to drop randomly below the atmospheric pressure as well (Figures A6 and A7). These observations led to a hypothesis, which suggests that the squeezing of the fibre pad between opposite bars of the plates creates strain in the fibre network under sealed conditions. This, in turn, may generate the under-pressure.

The first attempt to measure the pressure pulses in the refining zone gave, however, no clear conclusions because of some uncertainties associated with the sensors and the measurement system. First of all, some interference from the electrical grounding created offsets. However, the dynamic behaviour of the sensors seemed not to be disturbed because the results from the frequency domain obtained from the FFT analyses strongly indicated that the measurements gave process inherent information (Figures A7-A10). Secondly, two of the four tested sensors were made with a metal housing. These sensors were temperature dependent. However, preliminary tests strongly indicated that the temperature sensitivity was only significant in air and not in water. In addition a third sensor did not respond on pressure fluctuations at all because the sensor surface was assembled too far sub surface in the sensor housing.

Another weakness of the first trial was connected to the interpretation of the sinusoidal interferometric signal from the sensors. The sinusoidal transfer function between the raw signal and the pressures created uncertainty regarding the determination of the high pressure pulses. The uncertainty was associated to a physical phenomenon of interferometers, which is known as fringe counting. Eriksen (2003) showed how this phenomenon appeared in connection with similar pressure measurements in a high-consistency refiner. To overcome this limitation a slightly different sensor design was established before the latest trial. This resulted in improved readability, but the resolution was sacrificed. The last trial was in addition supported by an extensive investigation of the sensor performance in the Material Test System (MTS) Laboratory at STFI-Packforsk. The latter included tests where the sensors calibration curves were obtained. Results from these tests are shown in Appendix B.

4 Material and methods

4.1 Refiner

The refiner used in the present trials was a 600 mm (24 inches) Beloit Jones Double-D refiner in the series 4000 manufactured by Beloit-Walmsley Ltd. The refiner motor is frequency controlled, and thus variable speed is allowed. This refiner is driven by a 322 kW DC motor denoted DMA 315 S 35V from ABB Inc. The refiner has two flat stationary discs and a double-sided rotor disc in between. The rotor disc is movable on a spline shaft. One of the stator discs is movable by a frequency controlled motor, which sets a mechanical load in the desired disc position. The rotor is assumed to be equally balanced and positioned in the middle between the stator discs by the input flow of pulp suspension. This is not generally observed (Hammar (2005), Eriksen (2005)). It is assumed that the friction between the spline on the rotor disc and the spline shaft make this not to be obtained during all running conditions.

The refining system has one inlet tube, shown in Figure 3.1, and one outlet tube. In the present and previous trials the refiner has been operated as a single pass refiner. A rebuild of the system, operative from November 2005, allows up to 50 per cent recirculation flow into the refiner.

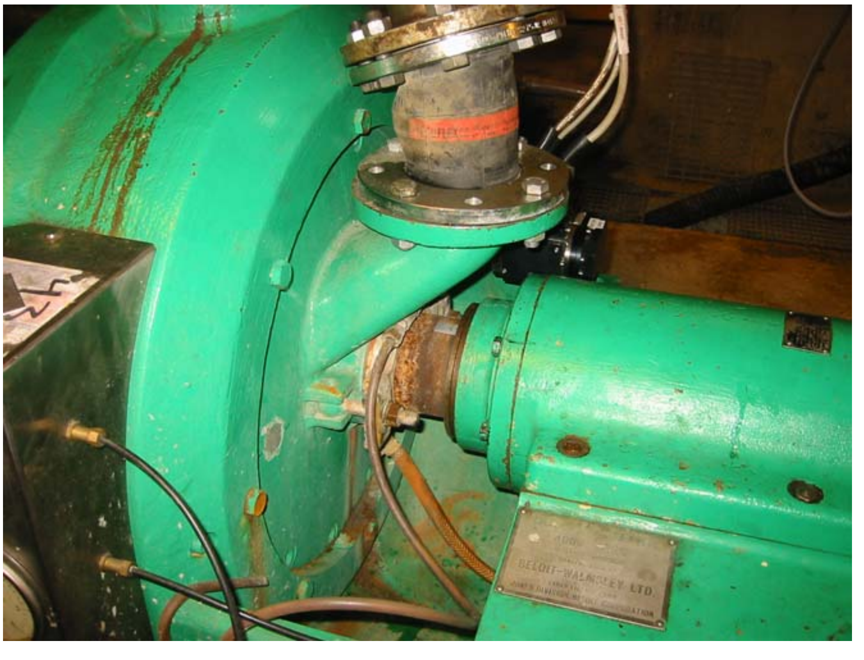

Figure 3.1. The photography shows the Beloit DD refiner seen from the fixed stator side. This stator door was replaced by another door incorporated the fibre-optic pressure sensors (Source: Ola Johansson, J&L Fiber Services Inc.).

The refiner system is equipped with flow and pressure controls. In addition, temperatures of the pulp suspension in and out of the refiner are measured and recorded together with other process variables in a distributed control system provided by ABB. In the same system plate clearance measurements are acquired. The latter is provided by Dametric AB. Their *Adjustable Gap Sensor* (AGS) is an automatic on-line self calibrating sensor for refiners. The sensor is a modified *True Disc Clearance* (TDC) sensor. Two sensors, located in each of the stator discs, have been tested in the present trials. Some results from these tests are shown by Eriksen 2005.

4.2 Plates

The present trial used one set of plates provided by J&L Fiber Services Inc. The plate and the design specification are shown in Figure 3.2. Additionally two more plate sets were used in the first attempt to measure pressure in the refining zone. A summary of the pulp quality development during changed process conditions is reported by Hammar 2005. That report contains results obtained from runs using different plate sets as well.

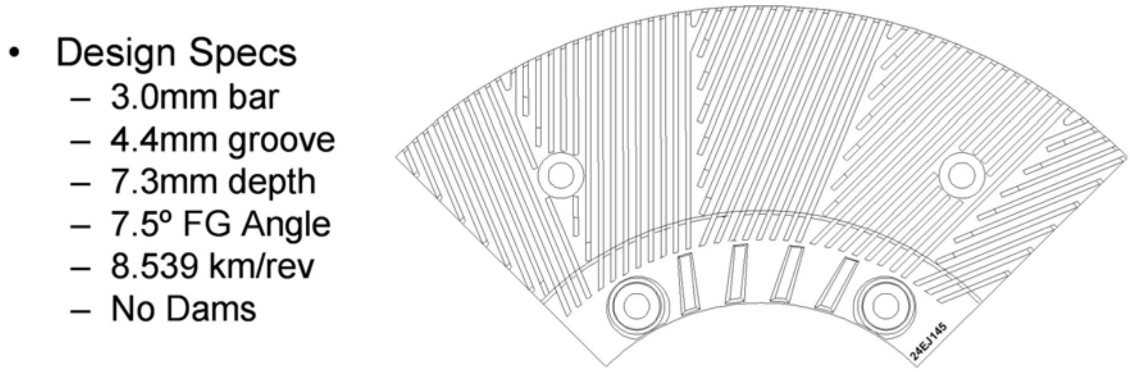

Figure 3.2. The applied plate and its design specification are shown (Source: J&L Fiber Services Inc.).

4.3 Running conditions

Several different running conditions are tested during the trial period. The trial plans for the refining of low-consistency refining of chemical and mechanical pulps are reported by Börje Svensson, STFI-PackForsk/EuroFEX (Svensson (2005a, 2005b)). The results shown in Appendix C are added with information about the prevailing running conditions.

4.4 Fibre-optic pressure sensors

Six fibre-optic pressure sensors were received before the second trial. These were further tested in advance as well as during refining of different pulps. The fibre-optic sensors from Luna Innovations, Inc. were mounted into the stator plates manufactured by J&L Fiber Services, Inc. as shown in Figure 3.3. The stator discs were equipped with similar plates as shown in Figure 3.2. No surface modifications of the plates, that kept the sensors, were necessary except for the small holes of approximately 1 mm in diameter through the bars.

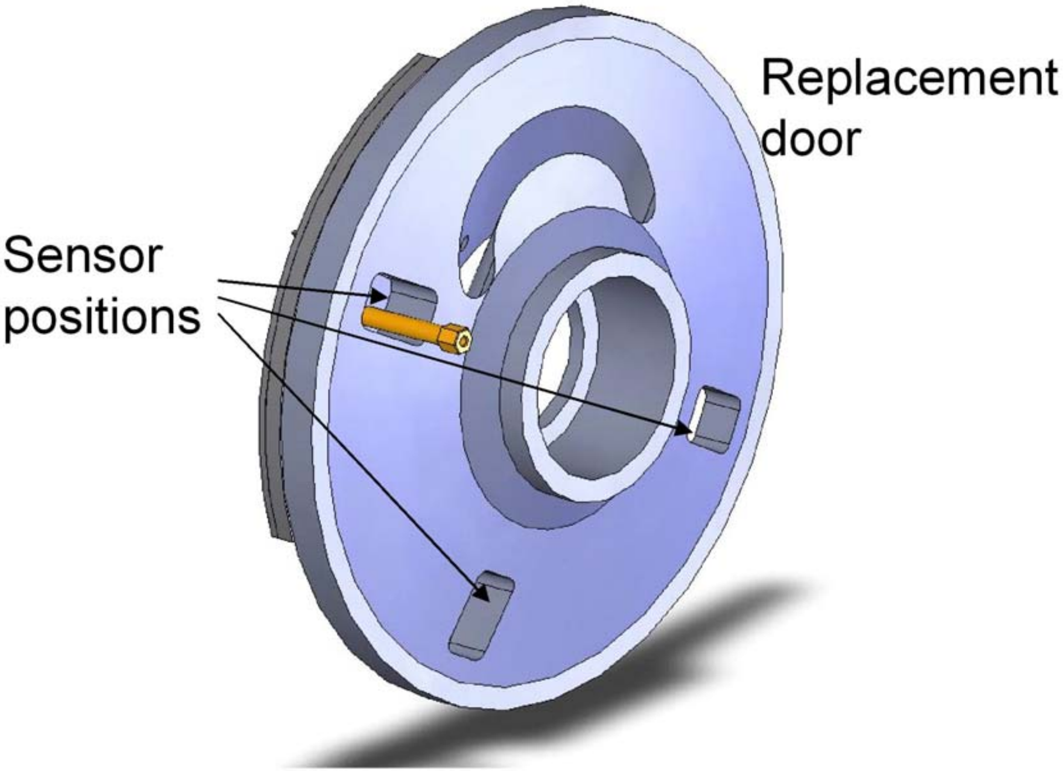

Figure 3.3. The stator disc equipped with three holes for the sensor holder. The latter is shown in the holes at the left hand side (Source: J&L Fiber Services Inc.).

The six fibre-optic sensors working basically as extrinsic Fabry-Perot interferometers were mounted into separate holes in the plates. Three sensors at the same time were mounted in the plates. It was prepared nine holes for the sensors in three main geometric positions in the stator disc as shown in Figure 3.3. Each of the main holes contained three sub-holes for the sensor holders. Thus, it was possible to place the sensors in slightly different radial positions in each of the three angle locations. The main angle positions were separated by 90°. The positions were 2, 5 and 8 o’clock respectively (or 60, 150 and 240°) seen from the rotor side. One of these main positions was omitted because the corresponding holes in the plate did not fit to the holes of the sensor holder in the stator disc. The reason for this was probably that the four refiner plates of the plate set had changed place compared to the original positions. Thus, the angle positions that were applied in the present trial were the positions at 150 and 240°. In addition two of the three sub-holes in each of the main positions were used. The corresponding radial positions were approximately 59 and 80 mm from the periphery of the plates.

Figure 3.4 shows a sketch of the pertinent plate where one of the sensors was located. The radial and tangential position of sensor 2 is indicated. Sensor 2 was located in this position, 59 mm from the periphery in the angle position 240°, during the whole trial. Thus, readings from sensor 2 have been investigated more intensively than the other sensors during this trial. The number of bars of the opposite rotor plates, which is passing the sensor is quoted above the bar pattern too. The number of bar and groove periods is divided in different sections of the plate separated by the two bolt holes as well as the flow channels separating the angled sections. This bar pattern and the open spaces associated with the bolt holes and flow channels were clearly visible in the pressure recordings.

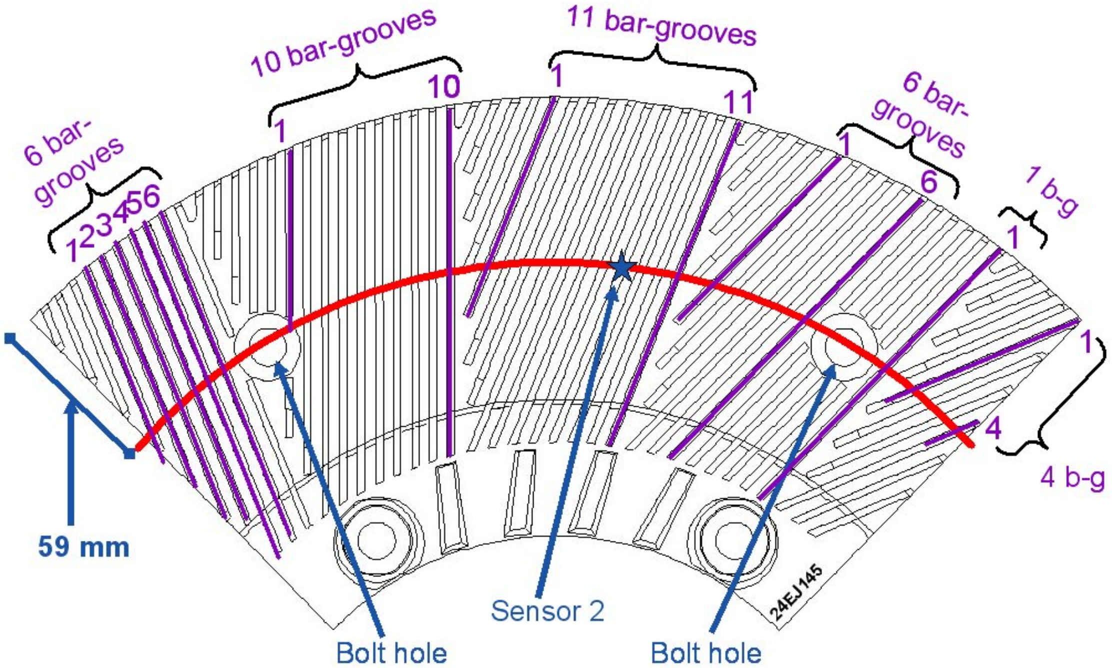

Figure 3.4. The radial and tangential position of sensor 2 was approximately 59 mm from the periphery in the middle part of the plate. The number of bars of the rotor plates passing the sensor location is indicated by the figures in the upper part of the sketch.

The sensing surface of the fibre-optic pressure transducers was about 1 mm in diameter. The transducers are called EFPI fibre-optic strain sensors. EFPI is the abbreviations for Extrinsic Fabry-Perot Interferometer, which is the functional principle of the sensors. In other words, the sensor is based on interference between reflected light waves. The output signal from the interferometer is the phase difference of the light that appear when the gap between the reflecting surfaces alters as a function of the pressure imposed on the sensor surface. One of the reflecting surfaces is the optic fibre itself and the other is the reflecting surface in the end of a sliding gap also called Fabry-Perot cavity, which the light is transmitted into. A sketch of the EFPI pressure sensor is shown in Figure 3.5.

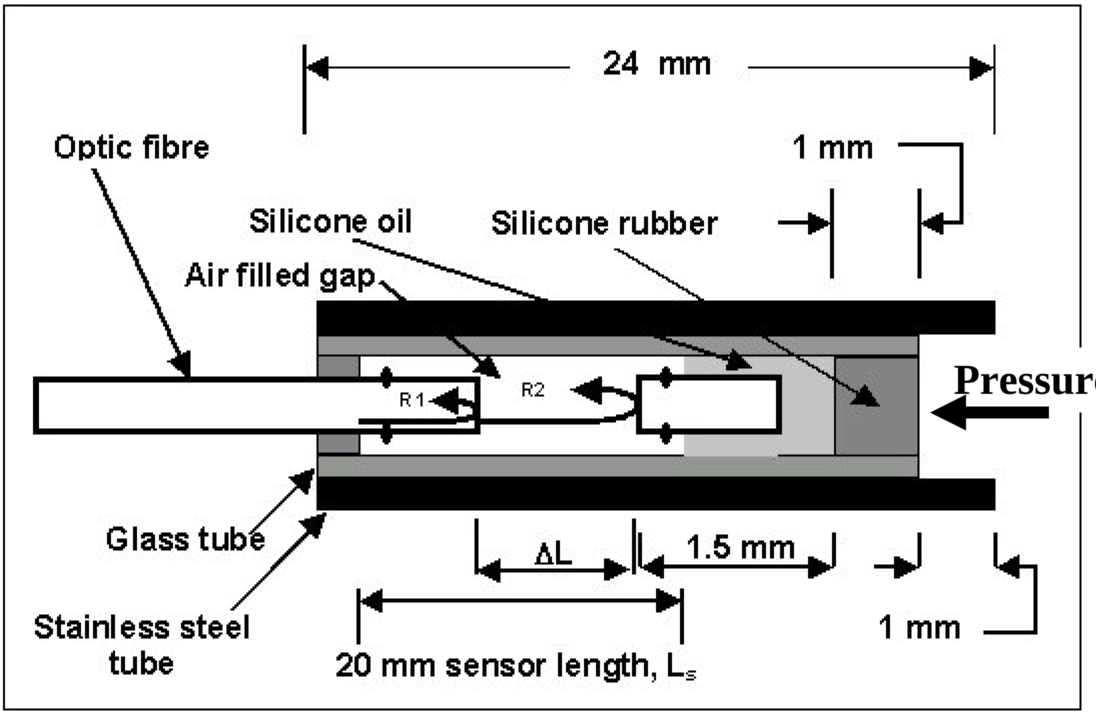

Figure 3.5. The principle sketch of the Extrinsic Fabry-Perot Interferometer pressure sensor as provided by Luna Innovation Inc. is shown (Eriksen (2003)).

The sketch in Figure 3.5 is basically a sketch of a similar sensor, which was used in corresponding experiments conducted in a high-consistency chip refiner (Eriksen (2003)). The dissimilarities between the present sensors and the earlier version of the sensor are the absence of the silicone rubber located at the sensing surface of the transducer as well as the glass tube of the sensor was separated from the stainless steel tube. The modified design replaced the short stainless tube by a much longer tube of some 15-20 cm. The fibre-optic cable was glued in the far end of the transducer tube such that the sensing head was kept clear of the tube. The long tube was in turn mounted into a sensor holder by a threaded end bolt. While the sensor holder was attached to the back plane of the disc by threads, the transducer tube was entered into the small diameter hole through the plate. The thread on the far end of the transducer tube was used to adjust the sensor head position such that this was almost evenly aligned to the bar surface of the plate. The inner diameter of the sensor holder was measured to be 1.9 mm while the transducer tube had an outer diameter of 1.6 mm. The “freely floating” sensor head and its fibre-optic cable are even smaller of some 1.0-1.2 mm. Moreover, the glass tube surrounding the primary sensor parts ensures that the fused silica fibres that constitute the Fabry-Perot cavity are aligned. The optical fibre within the alignment tube is free to float such that the surrounding tube does not have to deform for strain transfer to occur. It can be mentioned that the working part of a single modus fibre-optic cable contains two main parts. The core of the cable is only 9 µm wide. The light is transmitted through this silica core. To keep the light into the core a silica cladding of 125 µm in diameter is surrounding the core. The different refractive indexes of these silica units are fit to optimize the light transmission.

The EFPI system consists of a single mode laser diode operating with a wavelength of 1310 nm. The light from the laser diode illuminates the Fabry-Perot cavity through an optic coupler. The cavity is formed between an input single mode fibre and a reflecting single mode or multimode fibre. The glass tube aligns the input fibre and the reflecting fibre. For uncoated fibre ends, only a minor part of the transmitted light is reflected (4 % Fresnel reflection) at both ends of the cavity, thus the EFPI can be approximated as a two-beam interferometer. The first reflection denoted R1 in Figure 3.5, called the reference reflection, is independent on the applied perturbation. The second or the sensing reflection is denoted R2. This is dependent on the length of the cavity, which in turn is modulated by the applied pressure. These two reflecting light waves interfere provided that the path difference is within the coherence length of the source.

Either the intensity as a measure of the energy or the power of the light can be expressed as a simple function of the cavity length, which in turn is affected by the imposed strain from the pulp suspension in the refining zone. When the sensor surface is exposed to compressive forces the reflecting fibre moves such that the gap between the fibres decreases and the phase of the interfering light waves vary. The phase variation affects the light intensity of the light brought back to the detector and the amplifier. Hence, the EFPI sensor is a phase-based sensor providing differential rather than an absolute measurement. It requires demodulation of some form in order to extract meaningful information. The sensors were delivered with calibration curves such that the absolute pressure was possible to extract from the measurements. In addition calibration tests were conducted at the Material Test System laboratory at STFI-Packforsk as well.

The measurement system from Luna Innovations consisted of a laser diode light source and a photo diode, light-intensity detector, with supplementing devices as drivers and amplifiers. This system is called FOSS I, Fiber Optic Support System no. 1. Its output signal is a voltage signal proportional to the interferometric optical signal. The interferometric signal is a sinusoidal function of the pressure. However, the sensors provided for the last trial were made such that the sinusoidal pattern was not predominant as shown in Figure B1. In other words, the pressure range of the sensors was high such that the prevailing pressures in the refining zone were solely connected to one monotonically leading or trailing edge of the sinusoidal relationship. This is in contrary to the transfer function curves of the sensors provided for the first experimental pressure sensor attempt as shown in Figure A3.

The combined laser driver and light detector unit, FOSS I, is the central unit in the measurement system. The laser driver provides transmitted light of a very stable wavelength to the sensor heads, while the light (photo) detector converts and amplifies the reflected light intensity to a voltage output signal. The FOSS I unit had one incoming and one outgoing channel such that only one sensor could be tested at a time. The bandwidth of the amplifying unit is claimed to be approximately 250 kHz. The amplified signals were transmitted via coaxial cables to the data acquisition system. The latter was performed using a high-speed DAQ-card from National Instruments Corp. with the following data:

- Type: NI-6115
- Channels: 4
- Resolution: 12 bits
- Internal gain: 0.2-50
- Sampling rate: max. 10 million samples per second (10Msamples/s) on one channel or 1.25 Msamples/s simultaneous on 4 channels

The high-speed DAQ-card was running on a CompactPCI-bus using a standard PC with a hard disk capacity of approximately 80 Gbyte and an internal memory of 256 Mbyte. LabVIEW software from National Instruments was used together with the DAQ-system.

In addition to recording one pressure signal, the other channels on the DAQ-systems were mainly used to record supporting data. The supporting data were collected from the two gap measuring units in addition to an accelerometer attached to the refiner housing on the tail end of the refiner. The accelerometer measured the high frequency axial vibrations of the refiner. The different recordings were conducted simultaneously at the same high sample rate, which mainly was 1 Msamples/s.

4.5 Calibration tests

The fibre-optic sensors were tested and calibrated at Luna Innovations locations before they were fitted into the plate. The pre-calibration was done with a variable optical attenuator (JDC Optics Model 5500L) to ensure a fix originating output value. However, the inline optical attenuator reduced the resolution of the output signal, and therefore it was decided to omit this unit in the final setup. The drawback was that variations of the output signal due to optic loss linked to connection of the fibre-optic connectors when replacing sensors to the FOSS system gave offset values. Testing and calibration of the sensors were performed on site before installation of the plates in the refiner. Zero bar gauge pressure was tested as well as tests in the Material Test System laboratory at STFI-Packforsk. Some results from the latter tests are shown in Appendix B. Data from these pre-tests gave input to the subsequent transfer functions of the sensors.

The laboratory tests in the Material Test System equipment were performed both in advance and in posterity. Figure 3.6 shows a sketch of the test equipment. The tests conducted in advance were pre-tests, which leaded to a final test set-up. Three of the sensors (sensors 2, 3 and 4) were tested according to the following program:

- Stepwise hydraulic load test. The volume above the sensor surface was filled with water. The hydraulic load was changed in steps of 5 kN from 0 to 40 kN. The load was divided by an area of 50 cm^2 (∅ 79.8 mm). Thus, the pressure was raised from 0 to 8 MPa (80 bar) during the test.
- Pulse test. A semi-dynamic response test was conducted in the water filled container. The duration of the pulse was 10 milliseconds from no load conditions to approximately 35 kN and back to unloaded hydraulic pressure again.

- Ramp test. A corresponding test as the pulse test apart from that the load was kept at the high level.
- The latter two tests were also performed in an air filled container, while a layer of 10 water saturated sheets (30 g/m^2) made of chemical or mechanical pulps were laid on the container bottom. The sensor was aligned almost even to this surface (bottom of the container). The space between the surface and the sensor surface was measured by a slide calliper. Sensor 2 was tested when it was 0.37 and 0.05 mm below the surface as well as 0.13 mm above the container surface. The area of the sheets was smaller (28.2 cm^2 (∅ 59.9 mm)) than the area of the water filled container, and thus the maximum load of 40 kN provided by the test system corresponded to a higher pressure of some 14 MPa (140 bar).

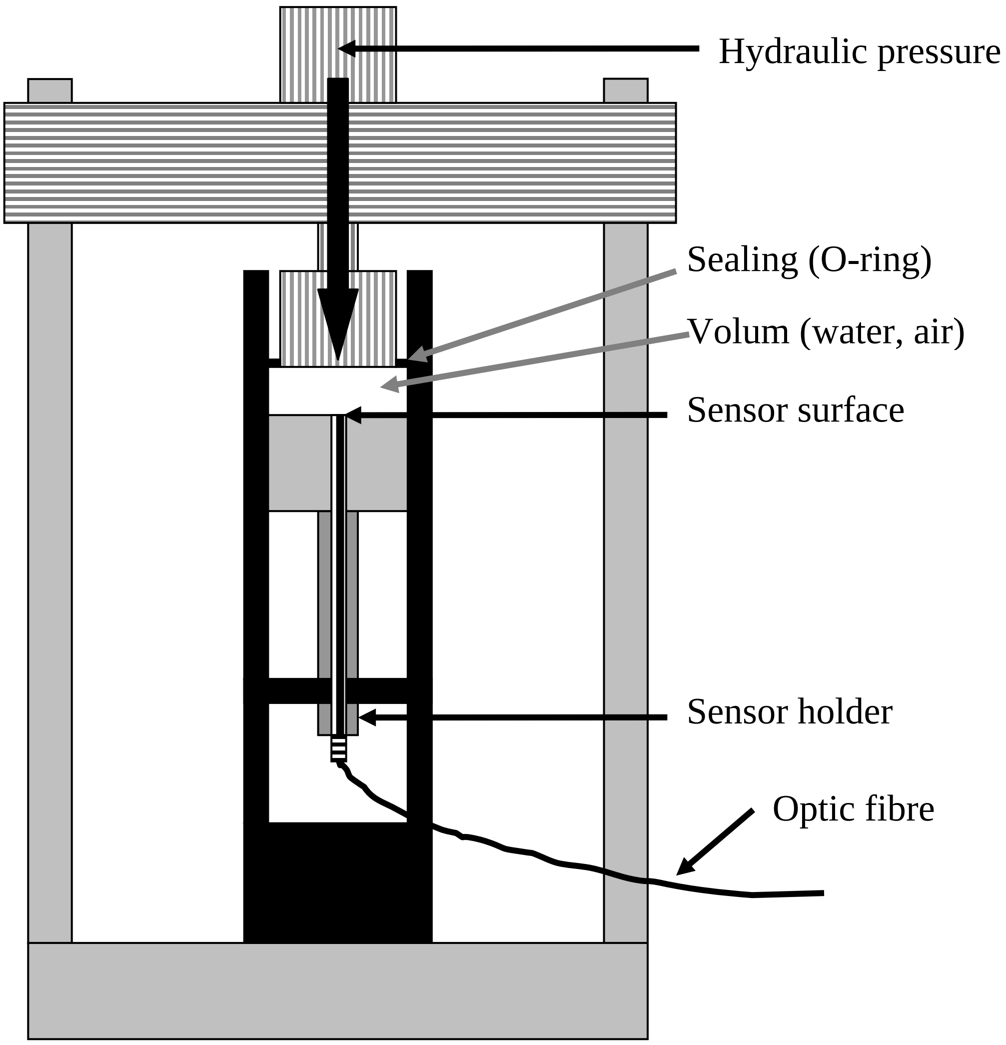

Figure 3.6. The sketch shows the test rig in the Material Test System Laboratory at STFI-Packforsk, which was used to test the response of the sensors.

The tests performed in the MTS laboratory clearly showed that the sensors responded ideal to pure hydraulic loads (Figure B1). The dynamic behaviour of the sensor was very good as well. The evaluation of the responses while a wet fibre pad was laid on the sensor surface showed that the fibre network supports parts of the applied load (Figure B3). The tests associated to the location of the sensor surface in the plate determined by the depth below the plate surface gave indications, as expected, that the depth should not be more than a few micrometers. Another observation done in the Material and Test System Laboratory during the calibration tests of the sensors resulted in speculations concerning a leakage flow of water in and out of the cavity surrounding the sensor head. This assumed leakage flow is associated with suction forces back and forth to a fibre mat under varying load because of the open cavity restricted by the transducer and the sensor tubes. This phenomenon is assumed to exist because the responses from the calibration tests where a set of water saturated sheets was above the sensor head during pressure pulse testing showed a time delay between the activating force device and the measured pressure. Figures B2 and B3 shows the corresponding measurements, which formed the foundations for these speculations. The existence of these forces and the corresponding leakage flows are not verified.

4.6 Data analysis methods

The recorded data were analysed using applications in LabVIEW and Matlab. The following part of this section describes the analyses that were made:

- Data were visually inspected and analysed statistically on data sets of 2 Msamples (2^{21} samples). This investigation was performed to get an overview of the different batches of samples and the sensors functionality.
- Histograms (*pmf*) and cumulative distributions of the recordings gave an overview of the distribution of the voltage output signals. The resolution of the histograms and distributions, which determined the number of bins, was mainly equal to the resolution (LSB) of the recorded time series.
- Frequency analysis was an important analysis method. The normalized amplitude spectrum analysis performed using FFT (Fast Fourier Transform) was used to find out if the output signals carried some periodic patterns. The normalized term was used to show the relationship between the amplitudes in the frequency domain with the corresponding amplitudes in the time domain. A unit sinusoid in the time domain corresponds to unit amplitude in the frequency domain. The FFT-routine in Matlab was used in the calculations.

5 Results and interpretations

5.1 High pressure pulses

Figure 4.1 shows high pressure pulses that occurred periodically at a rate corresponding to the bar and groove pattern of the plates of the rotating disc. This is illustrated by the sketch superimposed on the pressure curve. The pressure pulses revealed pressures above 2 MPa. However, the activity at this pressure level occurred infrequently as shown in Figure 4.2. This indicates that the gap area between the surface of the pressure sensor and the rotor bars was filled with compressed fibres or larger agglomerates of fibre bundles only on rare occasions. The measurements shown in Figures 4.1 and 4.2 are collected during refining of unbleached softwood Kraft pulp. Comparable pressure and process information are shown in Figure C9.

Actually, the last trial did not enhance the interpretations of the previous trial, which indicated pressure peaks up to 7 MPa. The number of high pressure peaks seemed to be fewer than in the previous trial too. The explanation of this difference may be that the sensors were different. The present sensors had poorer resolution, while the readability was improved compared to the previously used sensors. In addition, it can not be excluded that the location of the sensors in the plate i.e. the depth from the plate surface to the sensor surface might have created differences. Unfortunately, the positioning of the sensors was not exactly determined. Likely, it is necessary to determine the position down to an uncertainty of a few micrometers.

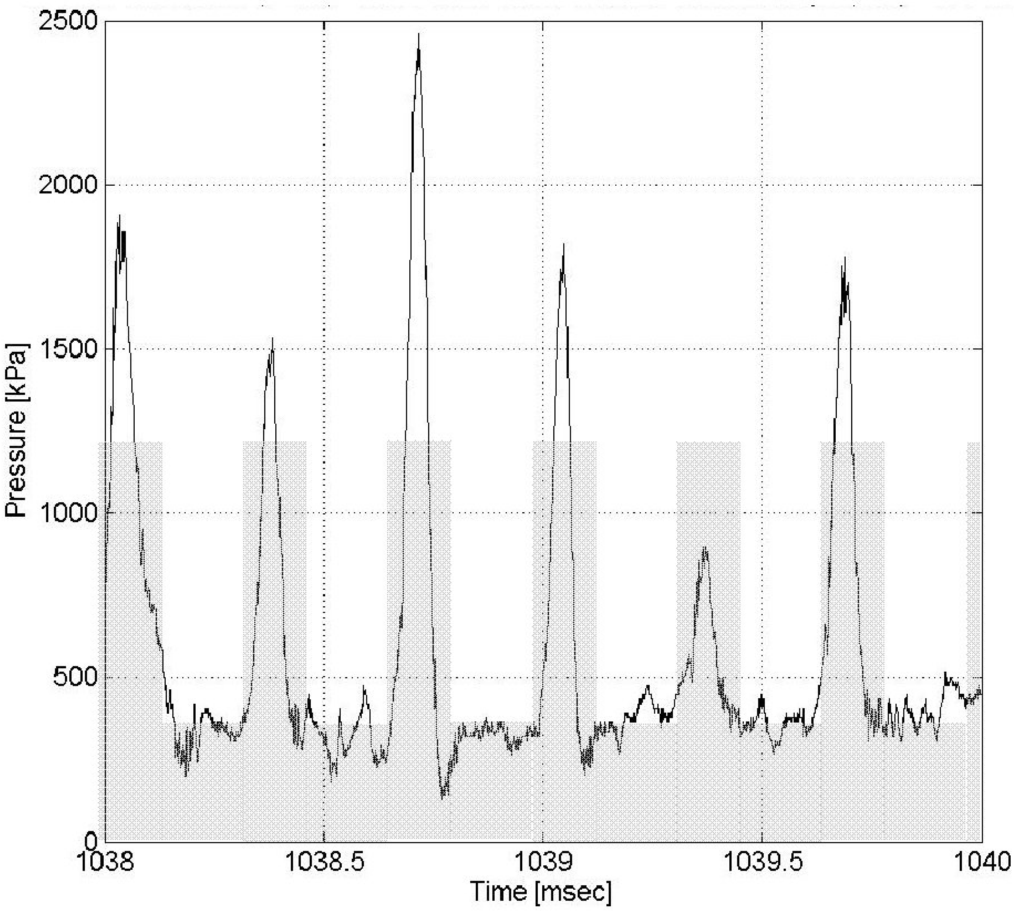

Figure 4.1. High pressure pulses versus plate geometry.

The recording shown in Figures 4.1 and 4.2 was not the typical pressure progress revealed in this trial. The phenomena shown in the following sections were more common. The main difference between this run and the others was the type of pulp that was used. Figures 4.1 and 4.2 show the pressure readings while unbleached softwood Kraft pulp was treated in the refiner. The pulp suspension in the other runs contained either bleached softwood Kraft pulp or high-freeness mechanical pulp. The distinction between these pulps is significant. The ability to build agglomerates of fibres is one of the distinctions. The unbleached softwood Kraft pulp contains more lignin compared to the bleached Kraft pulp. Thus, the fibres are probably much stiffer than the bleached fibres. The long and stiff fibres have larger ability to flocculate compared to the long and more flexible bleached softwood Kraft fibres and the short and stiff mechanical pulp fibres. This largely agrees with the assumption that the high pressure pulses are created by larger flocs of fibres trapped between the opposite bars in the refining zone.

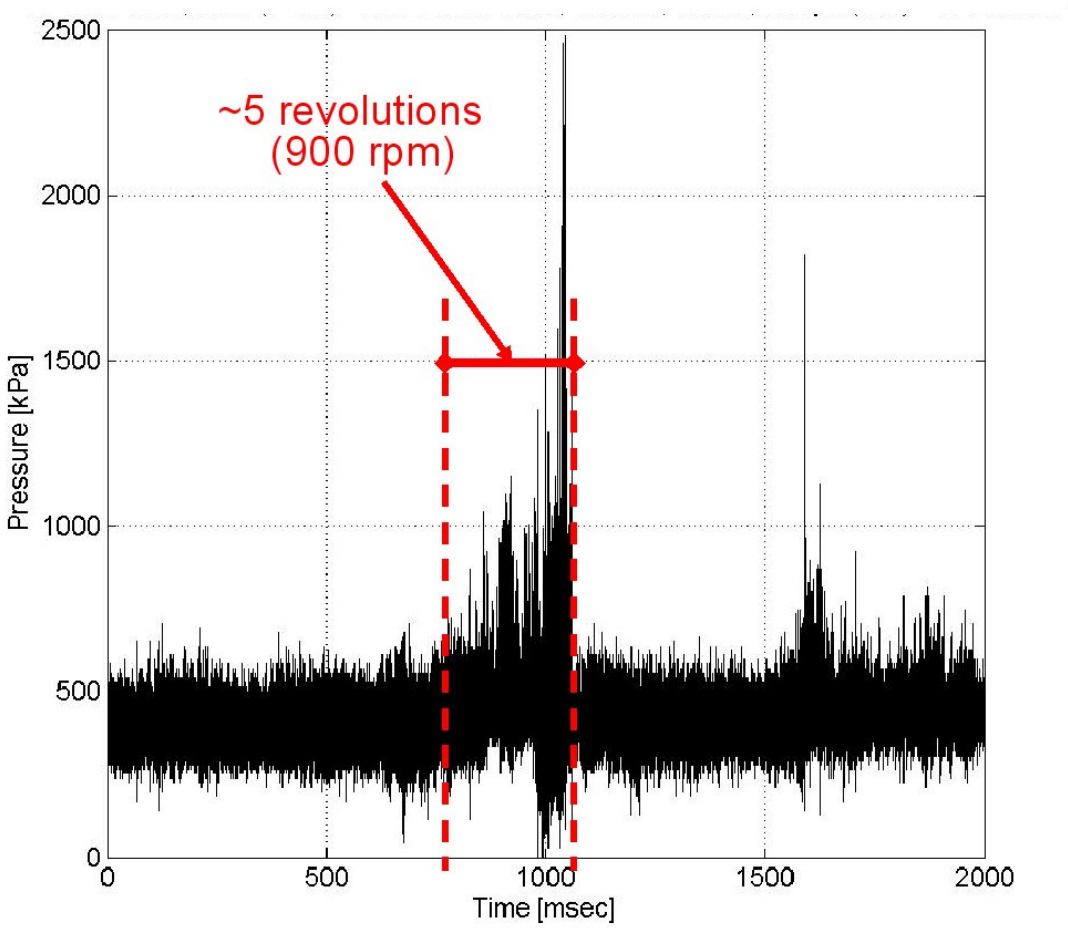

Figure 4.2. Few high pressure pulses are observed during this period lasting for 2 seconds.

5.2 Negative pressure and implosions

One of the most remarkable results obtained from the last pressure sensor trial was that pressure drops below an evident average pressure level were frequently observed. This is shown in Figure 4.3. Mainly, all of the recordings showed such pressure course, which can be associated to the passage of the bar and groove pattern of the rotating disc at the location of the pertinent sensor. The regularity of this pressure pattern is shown in Figure 4.4 where a drawing of the plate pattern is superimposed on the selected recording. The result strongly indicates that negative pressures (below atmospheric conditions) often appeared as well. The pressure drop was often followed by very high pressure spikes of short duration. The latter is interpreted as shock waves generated by implosions of vapour bubbles. No similar results from refining studies are ever reported. Figure 4.5 shows a pressure recording where these observations are clearly visible.

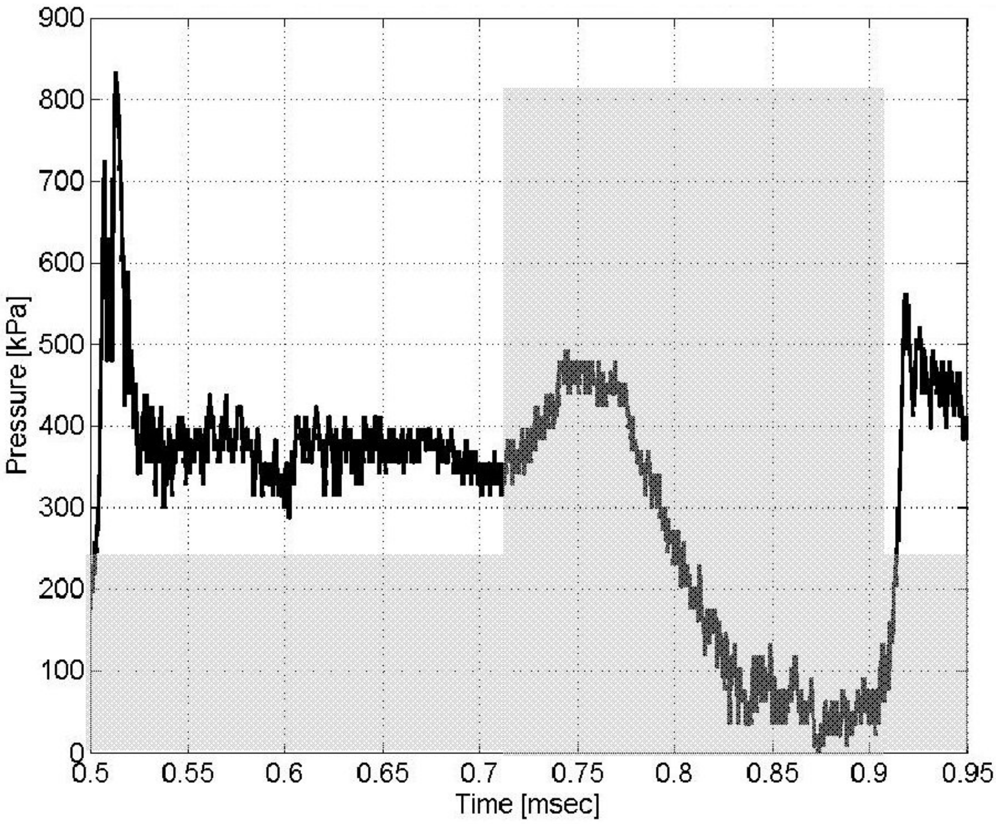

Figure 4.3. Pressure pulses versus bar and groove pattern superimposed on the recording.

Figure 4.3 shows a minor part of one recording from sensor 2 during refining of bleached softwood Kraft pulp. The sample rate was extremely high of 5 Msamples/s. Figure C1 shows a similar recording, which was collected almost at the same time and at similar operational conditions of the refiner. Figure 4.3 indicates that the pressure is approximately constant when a groove of the rotor disc is directly opposite the sensor surface. When the edge of a rotor bar is facing the sensor surface a pressure increase is observed. However, the pressure drops fairly rapid a few hundred kPa before the rotor bar leaves the sensor surface. Subsequently two different scenarios are observed as a result of that the rotor bar has moved away from the opposite position of the sensor surface. One of the scenarios shows that the pressure normalizes to a certain level. This is revealed in Figure 4.3 at the right hand side. The other scenario is shown at the left hand side of the figure where a substantial higher pressure spike appears. The latter may be associated with a shock wave caused by an implosion of a vapour bubble created by the negative pressure. The generation of such shock waves strongly indicates that cavitation effects are present in the low consistency refiner.

Figure 4.4 shows that the pressure fluctuations occur frequently, and that it happens as a consequence of the prevailing plate geometry at the location of the sensor. The rotational speed of the refiner determines the duration of each bar passage. The superimposed sketch of the plate pattern on the pressure recording strongly indicates that there is no coincidence when the pressure fluctuations occur.

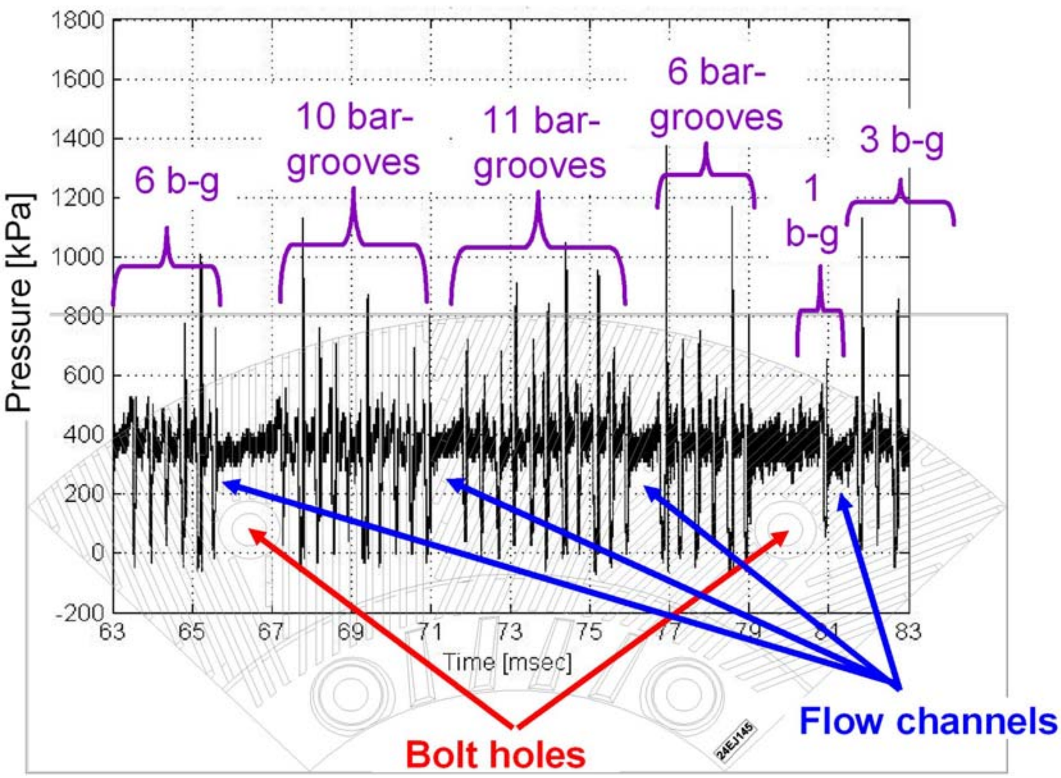

Figure 4.4. Pressure pulses versus plate geometry.

The pressure sensor was located approximately at the same radius as the upper part of the bolt holes of the plate. Thus, the pressure fluctuations were small when the bolt holes of the rotor plates swept across the sensor surface. This is actually shown in Figure 4.4. Additionally three more periods of less fluctuating pressures are visible. These are associated to the open flow channels in the plate which divides the plate pattern in sub-sectors. It is actually four sub-sectors per plate. However, the phase angel makes one-half sub-sector at each end of the plate to be divided between two adjoining plates. Each of the sub-sectors contains a number of bar and groove periods, which is evidently visible in the pressure recording. The number of bar and grooves, which is quoted in the upper part of Figure 4.4 is identical with the plate pattern illustrated in Figure 3.4. Moreover, Figure 4.5 shows an extracted part of the recording corresponding to one section of the angled plate pattern.

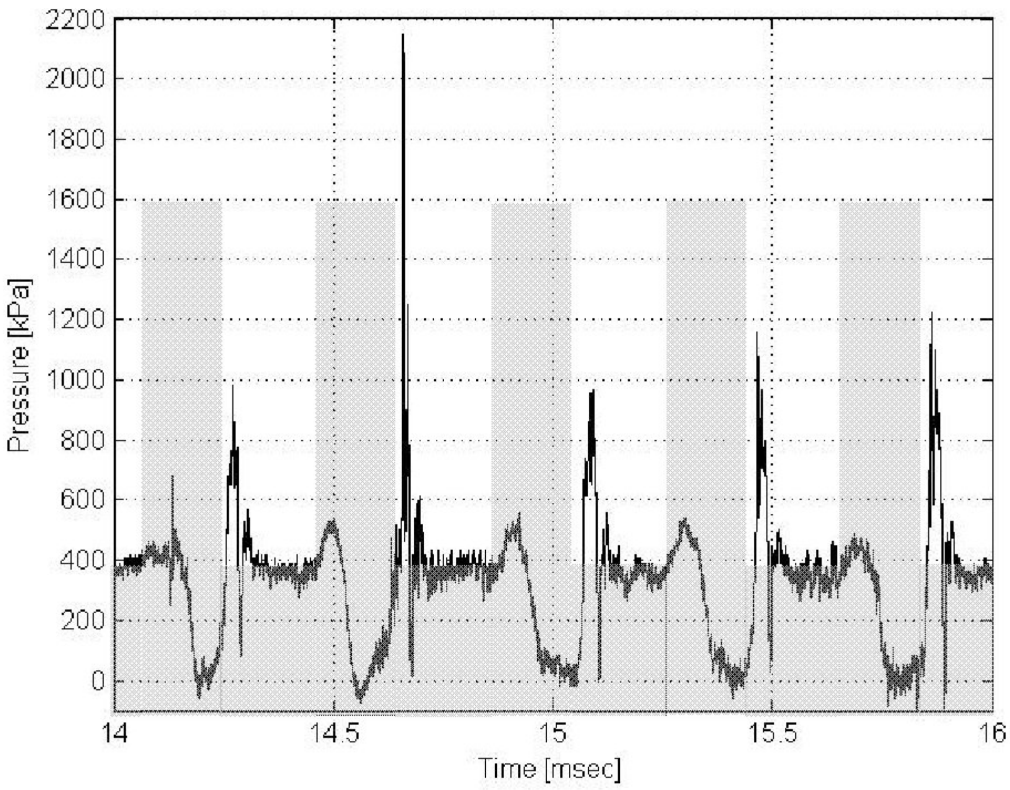

Figure 4.5. Pressure pulses versus five subsequent bar and groove passages.

Figure 4.5 reveals the connection between the negative pressures and the subsequent high pressure spikes, which is interpreted as shock waves. The prevailing transfer function between the raw signal, from the device that converts the optical signal from the interferometric sensor to a current or voltage signal, and the pressure indicates that the pressure drops below the atmospheric pressure. As a consequence of variations in the optical light intensity at subsequent reconnections of the fibre-optic cable to the amplifying device, a well-defined reference value is not obtained. Thus, the absolute pressure is hard to determine. However, this will only give different offset values at each reconnection. A try to track the offset values, which is based on several measurements at atmospheric pressure conditions before and after the fibre-optic cable was reconnected, gives indications that the offset can be in the order of a few hundred kPa. The sacrifice of the resolution in lieu of readability was a drawback in the case of determining the absolute pressure accurately.

The transfer function of the present sensor is provided from the calibration tests performed in the MTS laboratory as shown in Appendix B. The readings in Figure 4.5 are based on a transfer function added with a constant offset value of 260 kPa. Consequently, the overall average pressure was approximately 430 kPa for the recording of two seconds duration. This average pressure fits well with the casing pressure. However, the same recording is shown in Figure C1 with a lower offset value of approximately 140 kPa, which in turn makes the average pressure to fit the average value of the inlet pressure of the refiner. The latter is probably closest to the real value. The reason to claim this is a matter of fact that the cavitation effects should not be as evident as they are if the under pressure is not below a certain value. The vapour pressure of water is in turn determined by the temperature. The present recording was captured during running of bleached softwood chemical pulp at cold conditions. The temperature of the pulp suspension was only 28°C, which means that the cavitation effects should only be present when the pressure dropped below approximately 3-4 kPa absolute pressure (97-98 kPa below atmospheric). Moreover, refining of mechanical pulps at high temperature (85-95°C) exposes the refining process for even easier to become affected by undesirable cavitation effects. The pressure drop needed at this temperature is much smaller of some 15-40 kPa below atmospheric pressure. Figure 4.6 illustrates the basic mechanisms for the cavitation effect to occur.

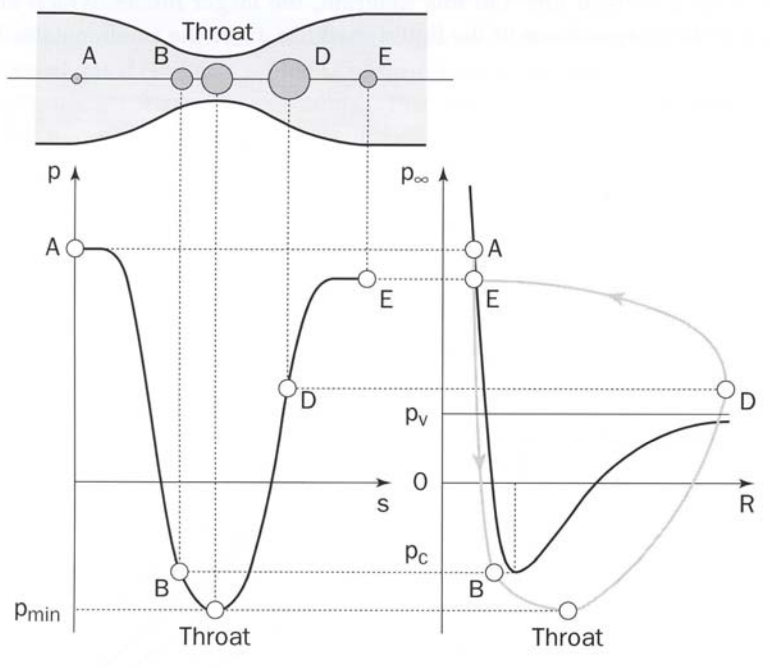

Figure 4.6. The illustration shows the growing of cavitations bubbles under influence of a decreasing pressure that can generate bubble collapse and subsequently shock wave propagation (Franc and Michel (2004)).

Figure 4.6 shows a typical evolution of a vapour bubble in a Venturi tube. This is an example which in turn can be associated to the narrowing passage in the gap between two bars in opposite discs. When the pressure decreases in the Venturi the vapour bubbles will expand. If the pressure drops below the vaporization pressure (p_c), which is dependent of the temperature, the vapour bubbles can grow unstable. The bubbles collapse when the vapour bubbles have passed the Venturi tube where the liquid medium has re-established the original pressure. This implosion generates shock waves, which might have destructive effects on the walls where the flowing medium is kept. In the case of refining, the shock waves can generate erosion wear of the refiner plates.

The overpressures due to the implosion of vapour bubbles can reach several thousand bars, and the duration of such collapse is extremely short. According to Franc and Michel (2004) the duration of a bubble collapse is in the order of one microsecond.

Figure 4.5 shows evidently that the shock waves have occurred, and thus the lowest pressure readings must have approached vacuum. It is not intended to determine the absolute pressures to a definite accurate level in this phase of the experimental work. In this state of the work it is important to investigate the performance of the pressure sensors and to derive whether the sensors are appropriate for this purpose. The objective is to verify the measurements and develop a final version of the sensor that gives reproducible recordings. At this stage of the investigation, it is accepted that negative pressures appear. The objective is to evaluate if the measurements are trustworthy, and furthermore how the negative pressures are created and in turn, which role the under-pressures might play in the refining of low-consistency pulp. Figure 4.7 are made to illustrate the current observations and form a hypothesis of what happens in the plate gap.

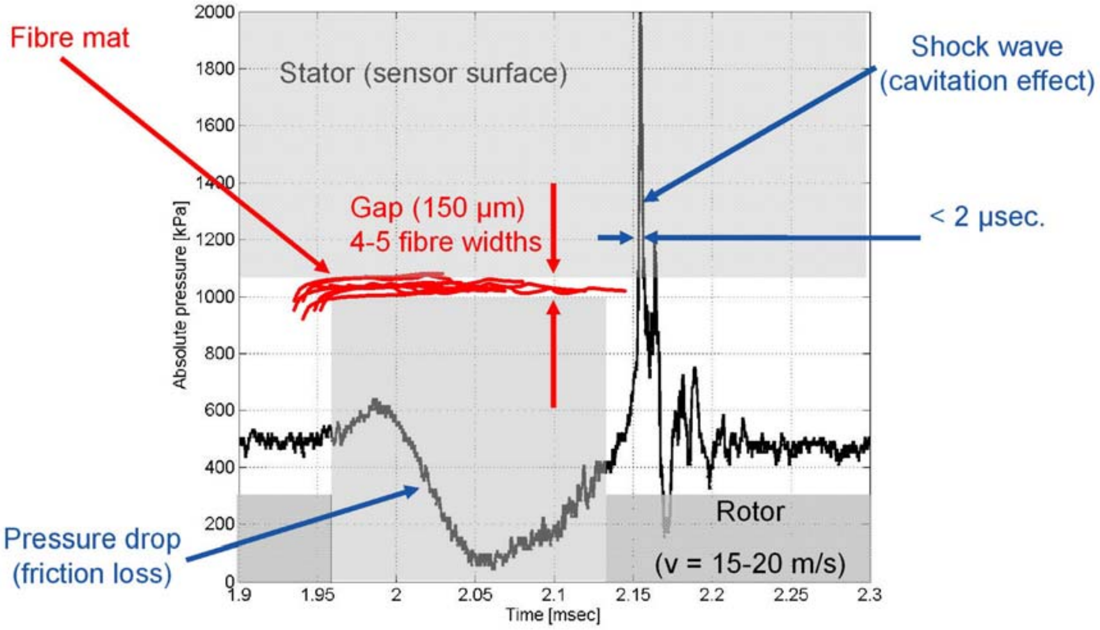

Figure 4.7. Pressure course through a bar and groove passage illustrated with a fibre mat squeezed in the small plate gap between opposite bars.

Figure 4.7 is based on a minor part of a pressure recording from sensor 2 during refining of softwood Kraft pulp. Corresponding readings are shown in Figure C1, but then with another offset value. The small part of the current recording consists of approximately 200 000 samples corresponding to the duration of one bar and groove passage. The assumed build-up of fibres on the rotor bar edge and bar surface is illustrated. The measures in this sketch are done accordingly to the scale values. Thus, the clearance between the bars of the stator and rotor discs (150 µm) is scaled to correspond to the width of the rotor bar (3.0 mm). Since the pressure recording is seen from the stator side it is necessary to evaluate the relative movement i.e. the stator moves while the rotor stands still.

Figure 4.7 reveals that the pressure increases during the first quarter of the rotor surface and drops during the next quarter. The pressure rise is probably due to the squeezing of the fibre mat. However, the increased pressure was unexpectedly small indicating that the pulp suspension did not create any large agglomerates of fibres that resisted the pulp flow through the small plate gap. Another important concern is associated to how well the pressure is measured in all positions of the rotor bar movement. It is important to be aware of the location of the sensor, which is in the centre of the stator bar. If it can be assumed that the pressure is largest at the leading edge of the rotor bar, it can be questioned how well the pressure is measured from the current location of the sensor.

The pressure drop, which followed the initial pressure rise, is assumed associated to the sliding friction (friction loss) of the fibre mat against the bar surface. The friction may also introduce strain in the fibre pad under sealed conditions, which in turn creates vacuum-like conditions. However, a velocity change of the pulp suspension through the plate gap might as well give a pressure drop. The latter may be interpreted that the pulp suspension are flowing radial outwards in the grooves influenced by a relative slow speed. When the pulp suspension is dragged into the gap between the opposite bars of the stator and rotor discs, the pulp suspension increases the velocity to the speed of the rotor disc as well as the flow direction is changed. The speed of the rotor disc is 15-20 m/s in tangential direction at the location of the sensors assuming that the rotational speed is in the order of 700-900 rpm. The velocity increase may introduce a pressure drop as well. Thus, both the sliding friction and the increased velocity might give a pressure drop. It is too early to conclude on which of these effects or a combination of the effects play the crucial role of the observed pressure drop.

The pressure recording in Figure 4.7 indicates that the pressure starts to normalize when the rotor bar is almost half way over the sensor surface. This may signify that the fibre mat is more loosely bond or on the contrary consolidated after approximately 1.5 mm. The former may be interpreted that the leading edge of the rotor bar tear up the agglomerate of fibres hitting it and thus, the remaining flocs of fibres flow more freely through the gap. By the meaning consolidate it is assumed that the fibre mat had restored a state of static equilibrium after the initial hit by the leading edge of the rotor bar. Anyhow, the measurements indicate that the contact between the fibres in the gap and the stator bar, where the sensor is located, was less aggressive since the pressure was re-established. Thus, it can be interpreted that the sliding friction decreased or that the pulp suspension velocity seen from the sensor side decreased. A slower pulp suspension velocity at the stator side of the plate gap compared to the corresponding velocity at the rotor side supports the assumption that laminar flow is the prevailing flow mechanism in the plate gap.

The last part of the recording in Figure 4.7 shows that the pressure in the pulp suspension was increased when the sensor sees the rotor groove. Figure 4.3 reveals that the pressure normalizes to an average pressure, while the recording in Figure 4.7 shows a development of the pressure that increases rapidly. The high pressure pulse is associated to the implosion of one or more vapour bubbles, which have been generated during the influence of the low pressure. The shock waves may disrupt any fibre mat that may exist. According to Franc and Michel (2004) dispersion of particles in a liquid medium can occur as a result of such cavitation effects.

The hypothesis that a fibre mat is sliding across the bar surface of the stator while it is more or less fixed to the leading edge of the rotor bar is an old theory. Already in 1919 a Dane named Sigurd Smith proposed such theory associated to a study of the action of the beater (Melby (1919), Stephansen (1967)). Stephansen, the inventor of the PFI mill, tested some of Smith's ideas. He demonstrated that the edges of the plate bars could collect a significant amount of fibre agglomerates with a consistency rising to 12 per cent. According to Page (1989), this effect was already in the 1950s called the ploughing term of friction. The theory was further enhanced by high-speed photography of stock transport in a disc refiner performed by Fox et al. (1979). In addition, an early attempt to measure the forces acting on fibres during a bar passage reported by Khlebnikov et al. (1969) and Gocharov (1971) indicated a significant pressure rise at the leading edge of the bar, which supports this theory as well.

This theory signifies that there are at least two different flow phases in the refining zone. One of the phases is connected to the flow phenomenon in the high volumetric groove area, while the other is associated with the small volumetric gap intersection area. The latter constitutes only of some 0.6-0.2 per cent of the available volume between the plates in the present study. The figures are based on assumed plate gaps in the order of 100-300 µm. Appendix D gives an overview of the calculations as well. In addition to the different flow phenomena, the density and the consistency of the pulp suspension must differ significantly between the two definite areas. The dry solid content of the fibre mat in the bar intersection area is probably fairly high and the consistency is probably not constant during the passage of the rotor bar area either. May et al. (1988) showed that the pulp pad thickness was proportional to the mass concentration denoted as mg/cm^2. At least equally interesting, the results revealed that the thickness turned to flatten out during exposure of an increased applied load in the laboratory press. This signifies that the density of the fibre pad approaches a saturated level without the ability to increase further. Calculations done in connection with the present study fitted unexpected well to the results obtained by May and his co-workers as shown in Appendix D. The calculations derived the mass concentration in the bar intersection area provided that the volume of intact fibres filled the entire gap area. The latter implies that the dry solid density is approximately 220 kg/m^3. The mass concentration associated to a gap clearance of 100-300 µm was calculated to be in the order of 2-7 mg/cm^2, while the corresponding measurements obtained by May et al. (1988) showed values between 3 and 9 mg/cm^2. May and his co-workers used the data to estimate the fibre coverage ratio of the bar intersecting area in high-consistency refining as well as the residence time of the pulp. They stressed that the comparison between the laboratory press data and the refiner data maybe is unrealistic because of the clear differences between the two processes. However, the importance of this experiment in view of theoretical knowledge of the refining process seems to be quite good. The reason why it is reported here is that the hypothesis associated to the treatment of the fibres in the small plate gap also in low-consistency refiners seems to support the assumption of a pretty high pulp consistency during the short time available under load. The effect this fibre mat exposes to during the bar to bar passage seems anyhow to create under-pressure, which may be tied to a generated strain in the fibre network under sealed conditions. This strain may in turn be traced in the pulp quality development through improved strength properties. Despite the importance of the latter topic it is assumed outside the scope of the present study.

5.3 Fluctuating average pressure

The results shown in the previous sections have focused on pressure recordings of relative short time periods in order to extract information of the pressure responses as a function of the refiner plate pattern. It is also important to evaluate other information that follows the pressure readings. The result extracted from the recordings shown in Figure 4.8 reveals what the pressure progress was on average basis during a time period lasting for six seconds.

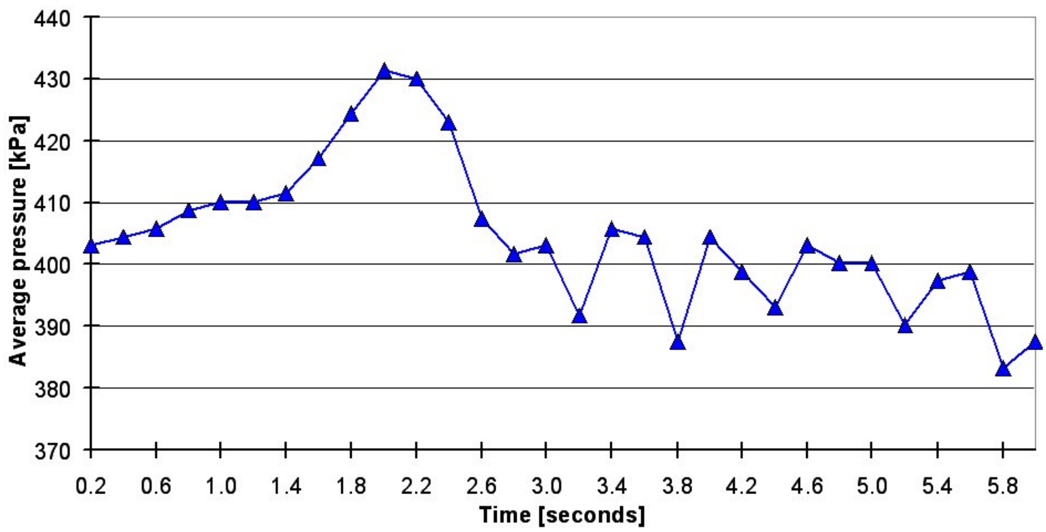

Figure 4.8. The average pressure in a 0.2 second window is shown for 30 subsequent periods.

Figure 4.8 shows a set of average values. Each point is the average pressure in a 0.2 second window (1 Msamples). 30 subsequent periods (30 Msamples) are shown. Corresponding process and sample information is quoted in Figure C1. The pressure progress indicates evidently trends in the recording. Figure 4.8 shows that the pressure increased slowly during a two-second period before it decreased. The pressure variation was approximately 30 kPa. As a comparison the external pressure variations in the inlet and the casing measured by ABB transmitters were only in the order of ± 2 kPa at the same time. This signifies that the internal pressure variations in the refining zone can be measured more accurate, which in turn gives the opportunity to deduce more information from such measurements than from commercial control system devices. The extended information can generate knowledge about the process that can be used to propose different approaches of for instance plate design and operational strategy. However, the causes for different observations, such as the relatively rapid and large pressure variations revealed in Figure 4.8, have to be analyzed before any efforts can be activated. Thus, Figure 4.8 is an example of what information that is accessible in the novel pressure recordings.

5.4 Frequency information

Figure 4.9 shows another example of information that is available in the pressure recordings. It is possible to extract process inherent properties by the use of frequency analysis of the recordings. The frequency plot in Figure 4.9 contains three main peaks originating from three different recordings.

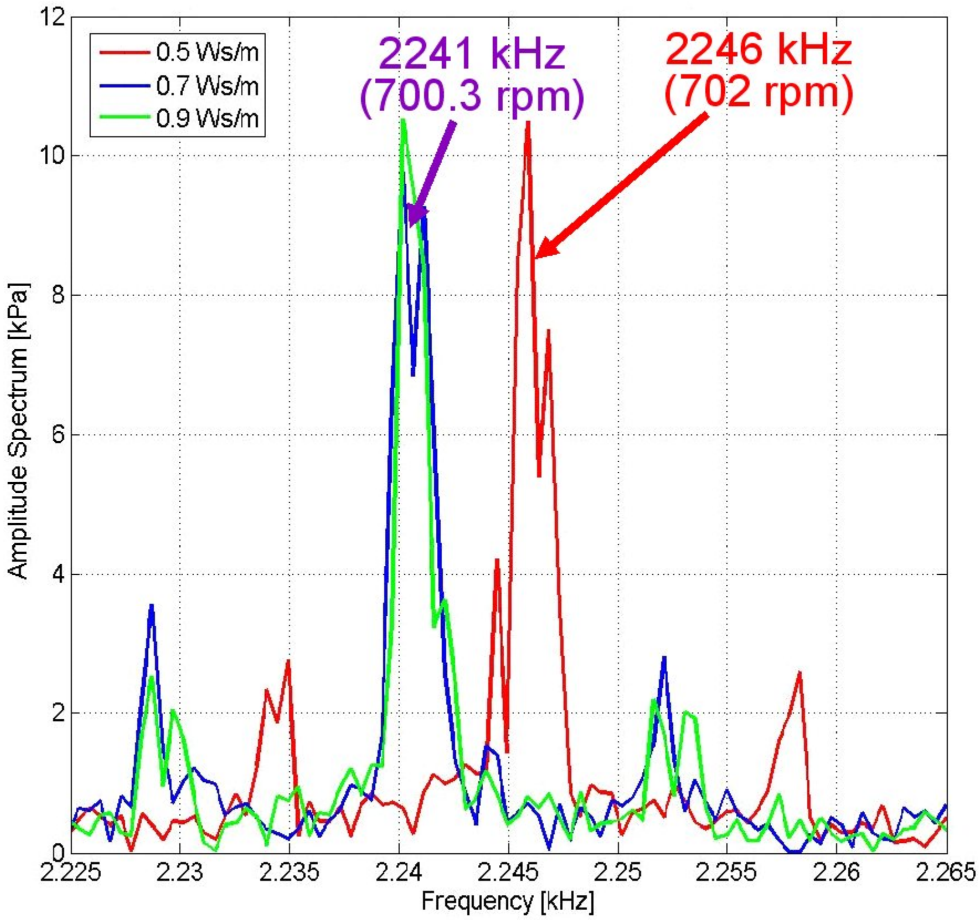

Figure 4.9. Amplitude spectra from three different recordings are shown. The peaks originate from the local bar crossing frequency.

The FFT analysis gives information of periodical occurrences in the recordings. The frequency peaks shown in Figure 4.9 had the largest amplitudes, which mean that the periodic pressure variation had the largest influence from the source associated to these peaks. The source in this case is the local bar crossing frequency that occurs 2240 times per second. The location of the sensor was at a radial distance from the centre of the refiner that contained 48 bars per plate (192 bars per revolution). The rotational speed of the refiner was initially 700 rpm (11.67 rps). 192 bars per revolution multiplied by 11.67 revolutions per seconds give 2240 bars per second. However, Figure 4.9 shows that the peaks appeared at 2241 and 2246 Hz respectively. That signifies that the rotational speed of the refiner was slightly different at different runs. The rotational speeds were 700.3 and 702 rpm respectively. Generally, the influence of the rotational speed seems to be randomized in this study. No systematic changes are found due to different edge loads flow rate or other operational conditions. This is contrary to what has been observed in high-consistency refiners (Eriksen (2003)).

Another difference between the measurements performed in the low-consistency refiner compared to similar measurements in the high-consistency refiner is that the local bar crossing frequency dominates the frequency spectra. The term local bar crossing frequency is associated with the frequency created by the passage of the number of bar and groove periods at the location of the sensor. The reason why the local bar crossing frequency dominates the frequency spectra recorded from the low-consistency refiner is probably because of all the water present. The water phase probably reduces the influence of pressure variations originating from other locations in the refining zone. Similar interpretations from pressure recordings in a high-consistency refiner indicate that pressure variations originating from particular locations in the refining zone are transmitted through the steam and high-consistency fibre suspension as well as the refiner housing. Thus, locally measured pressure variations in high-consistency refiner can be suppressed, while the pressure variations originating from other areas in the refining zone are visible. This strongly indicates that it is possible to identify the areas where the main refining activity occurs from different locations in the high-.consistency refiner. This is probably not the case for low-consistency refiners, and thus it should be beneficially to measure the pressure in different radial locations in the refining zone to identify if or where the area where the main refining activity happens. Measurements of vibrations in the refiner housing shows that the vibrations can be tracked to the outer part of the refining zone (Eriksen (2005). This strongly indicates that the main refining action occurs close to the periphery of the plates in the low-consistency refiner.

5.5 Strange water flow phenomenon

Figure 4.10 shows a strange pressure pattern or at least unexpected since the recording was collected during flow of water through the refiner. Water flow phenomena were not intended to be investigated in detail. However, at an incident a pressure recording was done shortly after the operator had to change the flow through the refiner from pulp to water simultaneously as the gap clearance was increased to avoid plate clash. It was unexpected that the pressure recording should give such unambiguous pattern, which is evidently determined by the plate design. More data and process information from the same recording is shown in Figure C5.

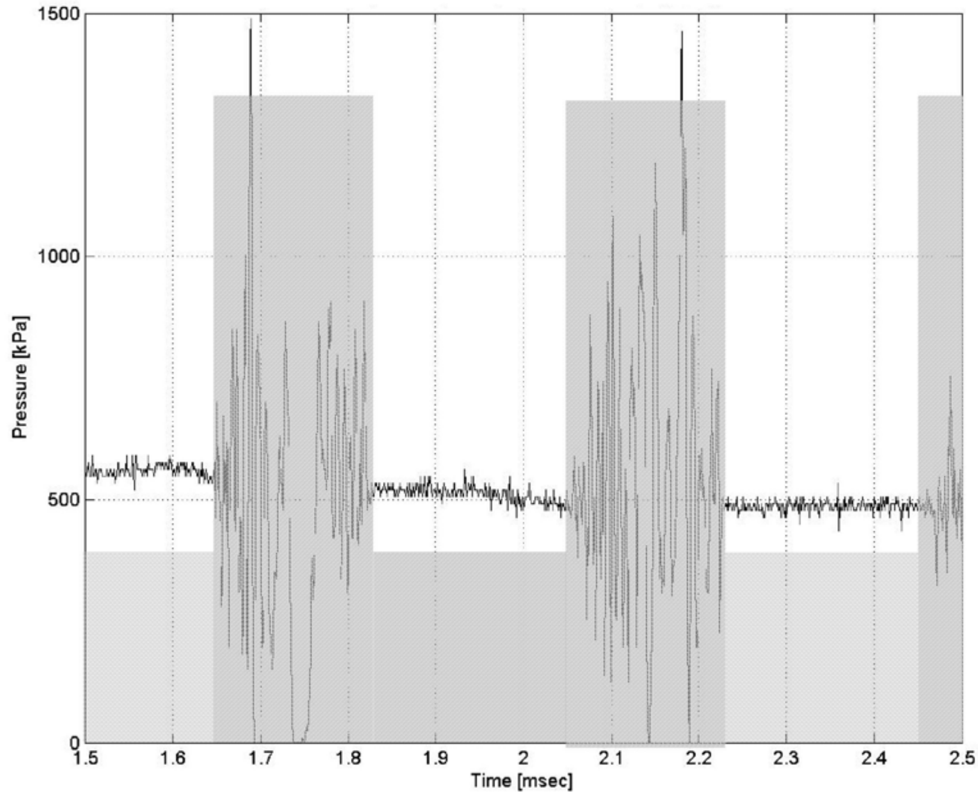

Figure 4.10. Pressure pulses in the refining zone recorded with only water present. The bar and groove pattern is superimposed on the recording to illustrate the different shape of the pressure pulses.

However, there are clearly differences between the pressure pulses in Figure 4.10 compared to the readings shown in the previous figures. The pressure pulses associated to the bar passage consist not of an expected progress as seen earlier. The pulses seem to be very rapid spikes of extremely short duration, while the pressure readings associated to the groove passages are contrary. The readings from the groove areas are smooth with small fluctuations about an average value indicating that the pressure was stable. The latter make this recording to be trustworthy. It is not expected that the rapid pressure pulses occur. The reason why these are visible may be found in the sensor location or in the design of the pressure transducer itself.

The location of the sensor was in a hole in a bar of the plate. However, the hole was made for the transducer tube. The sensor was mounted in the tube without no attachment points i.e. it float freely into the tube. The latter is correctly at the sensor head location. In the far end of the long transducer tube the fibre-optic cable was attached to the tube. The unattached sensor head may be influenced of a high shear flow when the water flows across the bar surface. The rapid pressure spikes may be results of this shear rate. Intuitively, it is possible that the sensor head was moving back and forth in the tube. Apparently, this movement may have caused the pressure readings. Thus, the readings are assumed false. To explain the rapid pressure spikes by physical descriptions has so far been unsuccessful.

The sensor design is proposed changed based on this strange observation along with another observation done in the Material and Test System Laboratory during calibration tests of the sensors. The proposal aims at fill the cavity between the sensor and the transducer tube with silicone. This will probably prevent any movements of the sensor head if such movements have taken place when the original sensor design was used. The new design will also prevent any leakage flow of water in and out of the cavity surrounding the sensor head. This assumed leakage flow is associated with suction forces back and forth to a fibre mat under varying load because of the open cavity restricted by the transducer and the sensor tubes. The existence of these forces and the corresponding leakage flows are not verified. The phenomenon is assumed based on interpretation of the responses from the calibration tests where a set of water saturated sheets was above the sensor head during pressure pulse testing of the sensor response. Figures B2 and B3 shows the corresponding measurements, which formed the foundations for these speculations and in turn the proposal of a modified sensor design.

6 Conclusions

The results obtained from this study have shown that the fibre-optic pressure sensors measure inherent properties associated with conditions in the refining zone. This is revealed by frequency analysis of the recordings. The frequencies of the bar and groove pattern at the location of the sensors dominated the frequency spectra. Variations in the local bar crossing frequency have been observed too. That signifies that the rotational speed of the refiner was slightly different at different runs. However, no systematic changes were found due to different edge loads, flow rates or other operational conditions.

The tests performed in the MTS laboratory clearly showed that the sensors responded ideal to pure hydraulic loads. Thus, the sensors ability to measure the pressure in the refining zone is to a great extent proved. There are still uncertainties connected to the measurement of the absolute pressures. However, the readability of the pressure readings was strongly improved compared to the first attempt to measure the pressure in the refining zone. The minor adjustment of the construction of the sensors that were applied in the two trials made it possible. Thus, the limitation associated with the demodulation of the pressure readings was conquered.

The most remarkable result obtained from the last pressure sensor trial was that pressure drops below an evident average pressure level were frequently observed. Mainly, all of the recordings showed such pressure course that occurred frequently at a rate corresponding to the passage of the bar and groove pattern of the rotating disc. The results strongly indicate that negative pressures often appeared as well. The pressure drop was often followed by very high pressure pulses of short duration. These rapid pressure spikes are interpreted as shock waves generated by implosions of vapour bubbles, which are generated by the observed under-pressures. The generation of shock waves strongly indicates that cavitation effects are present in the low consistency refiner. No similar results are ever reported

The initial pressure increase that appeared before the pressure drop was smaller than expected. The pressure rise was probably caused by the squeezing of the fibre mat between the bars on the rotor and stator discs. If the readings are true the accumulation of fibres and the corresponding impacts on the fibres from the bar surfaces, are probably less harsh than expected. However, another important concern is associated to how well the pressure is measured in all positions of the rotor bar movement. The location of the sensor was in the centre of a stator bar. If it can be assumed that the pressure is largest at the leading edge of the rotor bar, it can be questioned how well the pressure is measured from the current location of the sensor.

Some results show high pressure spikes that occurred periodically at a rate corresponding to the bar and groove pattern of the plates of the rotating disc. The pressure pulses revealed pressures above 2 MPa. However, the activity at this pressure level occurred infrequently. This indicates that the gap area between the surface of the pressure sensor and the rotor bars was filled with compressed fibres or larger agglomerates of fibre bundles only on rare occasions. The present trial did not enhance the interpretations of the previous trial, which indicated pressure peaks up to 7 MPa. The number of high pressure peaks seemed to be fewer than in the previous trial too. The explanation of this difference may be that the sensors were slightly different or that the running conditions of the refiner were different. The latter is not likely the reason despite the trials were run at different times. No major differences were introduced in the second trial. However, it can not be excluded that the location of the sensors in the plate i.e. the depth from the plate surface to the sensor surface might have created differences. A weakness with the trials was that the positioning of the sensors was not exactly determined.

There are only observed minor differences between pressure readings from different running conditions. The use of different type of pulps has not given any large deviations in the pressure measurements either. Refining of unbleached softwood Kraft pulp seemed to give a higher rate of high pressure pulses compared to the use of bleached softwood Kraft pulp and mechanical pulps. This is assumed explained through the ability of this pulp to flocculate. The high pressure pulses are probably created by the squeezing of larger agglomerates of fibres between the bars of the opposite discs.

Some unexpected pressure readings were also observed when water was pumped through the refiner. The pulses seemed to be very rapid spikes of extremely short duration. This occurred only when the bar intersection area was present. The pressure readings associated with the groove passages were indeed very smooth indicating that the overall performance of the sensors was proper. The reason why these rapid pressure fluctuations appeared may be found in the sensor location or in the design of the transducer itself. Intuitively, it is possible that the sensor head was moving back and forth in the transducer tube influenced by high shear forces. This movement may have caused the apparent pressure readings.

7 Further work

The present study has revealed some uncertainties regarding the sensor design as well as the assembly of the sensors in the plate. The observations have also disclosed some physical conditions associated to the fibre network and the pulp suspension that are still not explained. It is desirable to exclude any uncertainties and to deduce the unsolved questions by new experiments.

The sensor design is proposed changed based on the odd observation during pumping of water through the refiner along with the observation associated to leakage flows in the transducer tube. The proposal aims at fill the cavity between the sensor and the transducer tube with silicone. This will probably prevent any movements of the sensor head if such movements have taken place. The new design will also prevent any leakage flow of water in and out of the cavity surrounding the sensor head. However, the existence of these forces and the corresponding leakage flows are not verified. Thus, a modified sensor design is desirable to exclude any uncertainties connected to the sensors performance as well as the measurements. It is also required that the readability and the resolution of the measured signal are optimized in order to determine the absolute pressure more accurately.

The pressure response dependency of the location of the sensor surface in the plate determined by the depth below the plate surface should be evaluated more profoundly. It is necessary to determine the position down to an uncertainty of a few micrometers. However, another important concern is associated to how well the pressure is measured in all positions of the rotor bar movement because of the location of the sensor in the centre of the stator bar. The possibility to assemble the sensors in different locations of the bar width should be evaluated as well. In addition, obtaining the pressure response from sensors located in different radial locations of the plate is important in order to evaluate where in the refining zone the main refining activity occurs. The latter can be used to derive fundamental refining mechanisms through theoretical calculations of the impact intensities and the power consumption.

The unanswered questions regarding the physical conditions of the ability of the fibre network to support parts of the applied load should be investigated further. It is desirable to evaluate how relevant an effect like this is regarding the conditions in the plate gap. Also the observation associated with the pressure drop should be investigated in order to deduce the real mechanism behind this phenomenon in the plate gap.

Further work should also focus on the determination of unique properties of the pressure measurements at different operational conditions including refining of different type of pulps.

8 References

Fox, T.S., Brodkey, R.S. and Nissan, A.H.(1979): *"High-speed photography of stock transport in a disk refiner"* Tappi, 62 (3), pp. 55-58.

Franc, J.-P. and Michel, J.-M. (2004): *"Fundamentals of cavitation"* Kluwer Academic Publisher, Dordrecht, The Netherlands, 289 p., ISBN: 1-4020-2232-8.

Goncharov, V.N. (1971): *"Force factors in a disk refiner and their effect on the beating process."* Bumazh. Prom., 5, pp.12-14.

Eriksen, O. (2003): *"High-frequency pressure measurements in the refining zone of a high-consistency refiner"*, Doctoral thesis, Department of Energy and Process Technology, Norwegian University of Science and Technology, 50(04), 303 p., ISBN: 82-471-5601-6.

Eriksen, O. (2005): *"Mechanisms in the refining zone for development of physical properties of TMP fibres in a low-consistency refiner. High frequency vibration and gap measurements"*, Technical report STFI-Packforsk (in print).

Hammar, L.-Å. (2004): *"LC refining mechanisms – Literature review"*, STFI report MEC 42, 21 p.

Hammar, L.-Å. and Eriksen, O. (2005): *"Literature survey of potential measurement techniques suitable for the refining zone of disc and conical LC refiners"*, Technical report STFI-Packforsk (in print).

Hammar, L.-Å. (2005): *"Mechanisms in the refining zone for development of physical properties of TMP fibres in a low-consistency refiner. Plate pattern, plate clearance and pulp quality"*, Technical report STFI-Packforsk no. 108, 29 p.

Khlebnikov, A.A., Pashinskii, V.F., Goncharov, V.N. and Smirnova, E.A. (1969): Analysis of forces involved in the operation of a conical refiner, Bumazh. Prom. 22, pp.129-136.

May, W.D., McRae, M.R., Miles, K.B. and Lunan, W.E. (1988): *"An approach to the measurement of pulp residence time in a chip refiner"* J. Pulp Pap. Sci., 14 (3), pp. J47-J53.

Melby, B. A.(ed.) (1919): *"Ny literature. Heltøyshollænderen"*, Papir Journalen, 8(4), pp. 23-27.

Page, D. H. (1989): *"The beating of chemical pulps – the action and the effects"* Fundamentals of papermaking. Transaction of the 9th Fundamental Research Symposium, Cambridge, UK, Vol 1, pp.1-38.

Stephansen, E. (1967): *"Bidrag til belysning av maleprosessens mekanisme"* Norsk Skogindustri, 21(8), pp. 266-275.

Svensson, B. (2005a): *"Uppdrag vid EuroFEX. Projectplan. Malning AFM, vecka 21-22, 2005"*, STFI-Packforsk Projectplan 286-12-50, 5 p.

Svensson, B. (2005b): *"Uppdrag vid EuroFEX. Projectplan. LC-malning av TMP og RTS, vecka 22, 2005"*, STFI-Packforsk Projectplan 286-12-60, 9 p.

Appendix A:

Measurement results obtained from the first pressure sensor trial in the fall 2004

Fibre-optic pressure sensors – short description and evaluation:

MS1: Type: EFPI pressure sensor with metal housing
Measured pressure pulses: > 15 bar (the range of one sinusoidal flank)
Dynamic properties assessed to be good
Unstable static measurements (deviations between pre-calibration and readings, different readings at reconnection to the amplifier unit)
Temperature dependent (significant in air not in water)

LF1: Type: EFPI pressure sensor with long fused glass housing
Measured pressure: > 10 bar (the range of one sinusoidal flank)
Satisfactorily dynamic behaviour
Temperature independent

LS7: Type: EFPI pressure sensor with metal housing
Measured pressure: > 20 bar (the range of one sinusoidal flank)
Satisfactorily dynamic behaviour
Unstable static measurements
Temperature dependent

SF1: Type: EFPI pressure sensor with short fused glass housing
Measured pressure: only static pressure (located too far sub surface in the sensor housing to measure the pressure fluctuations)
Temperature independent

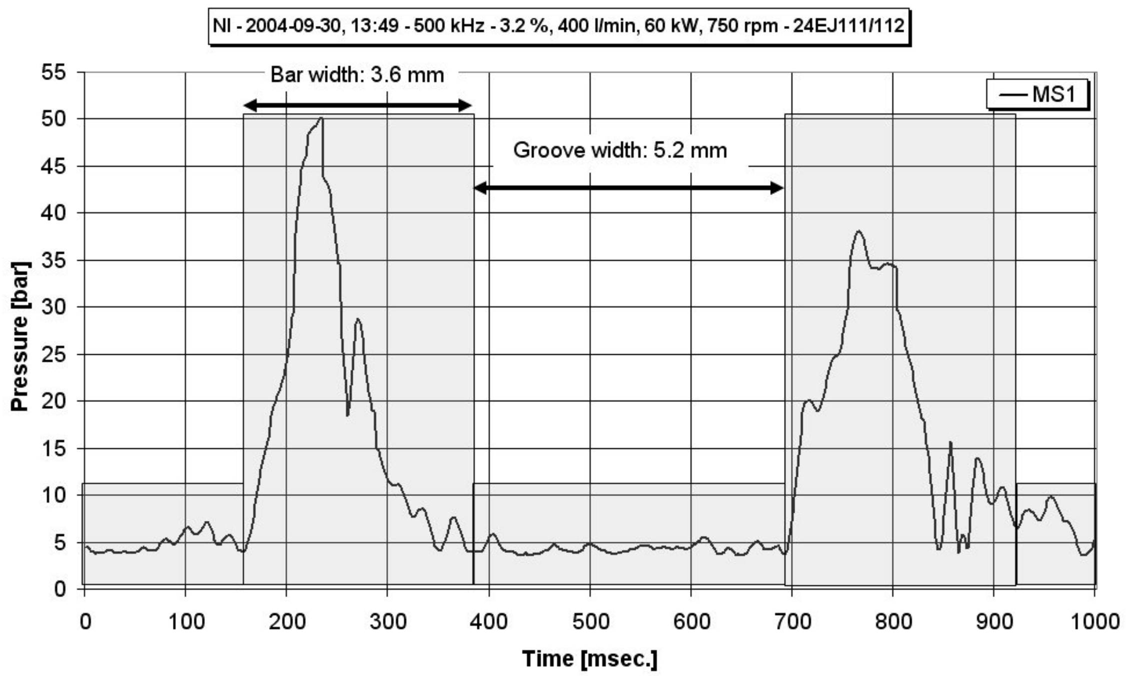

Figure A1: Assumed pressure response from sensor MS1 during refining of bleached softwood Kraft pulp.

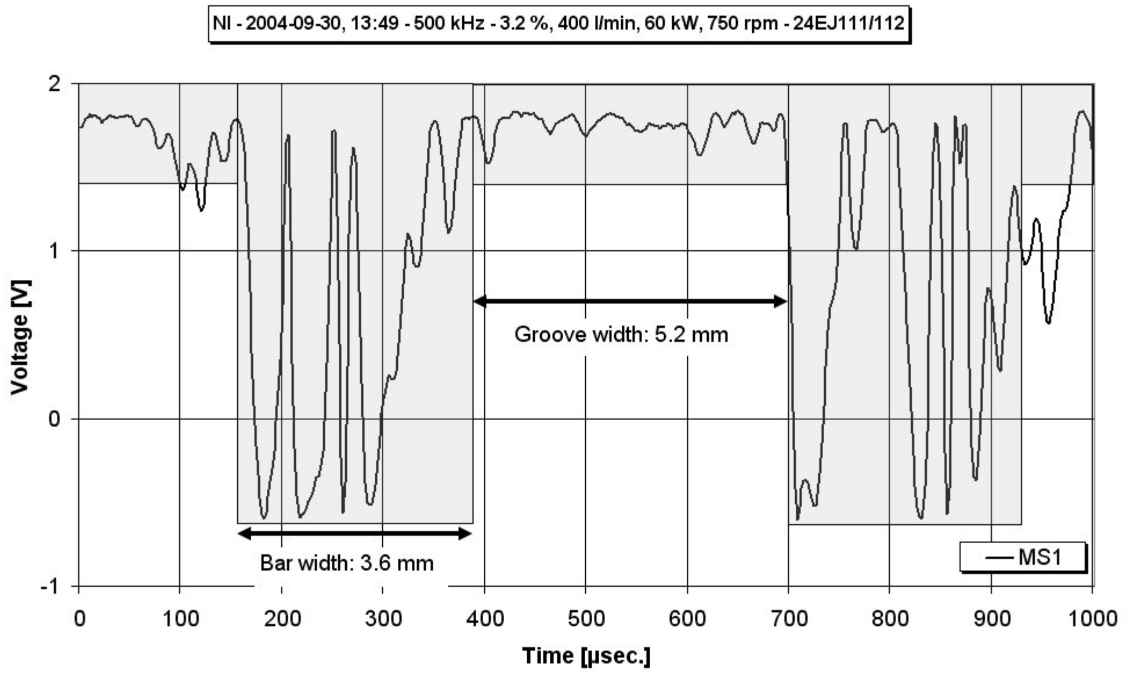

Figure A2: Raw data from sensor MS1 corresponding to data shown in Figure A1.

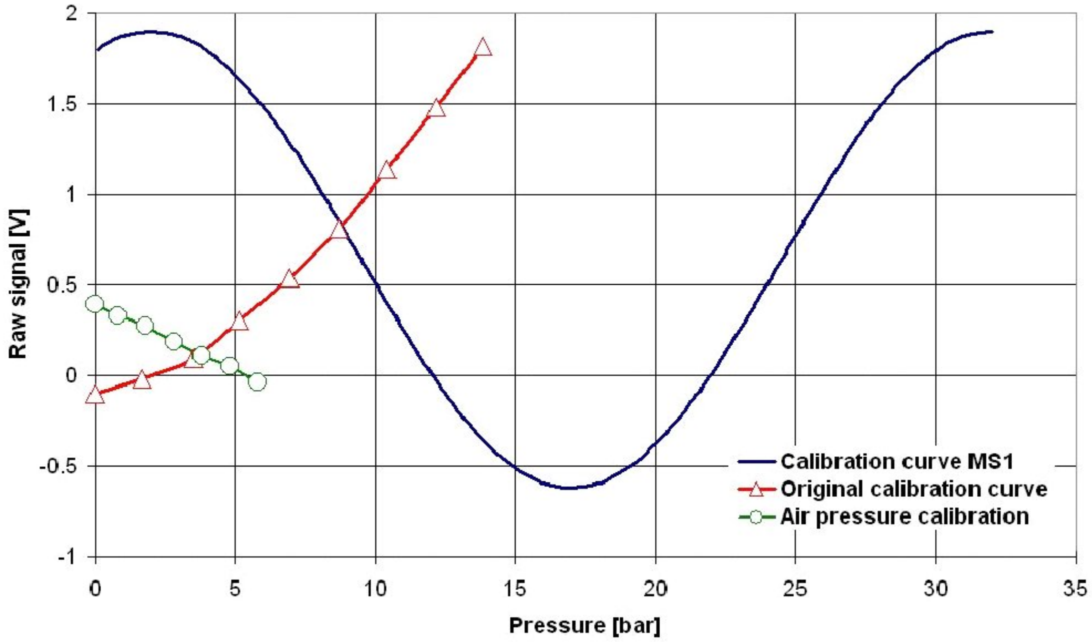

Figure A3: Transfer function curves obtained for pressure sensor MS1.

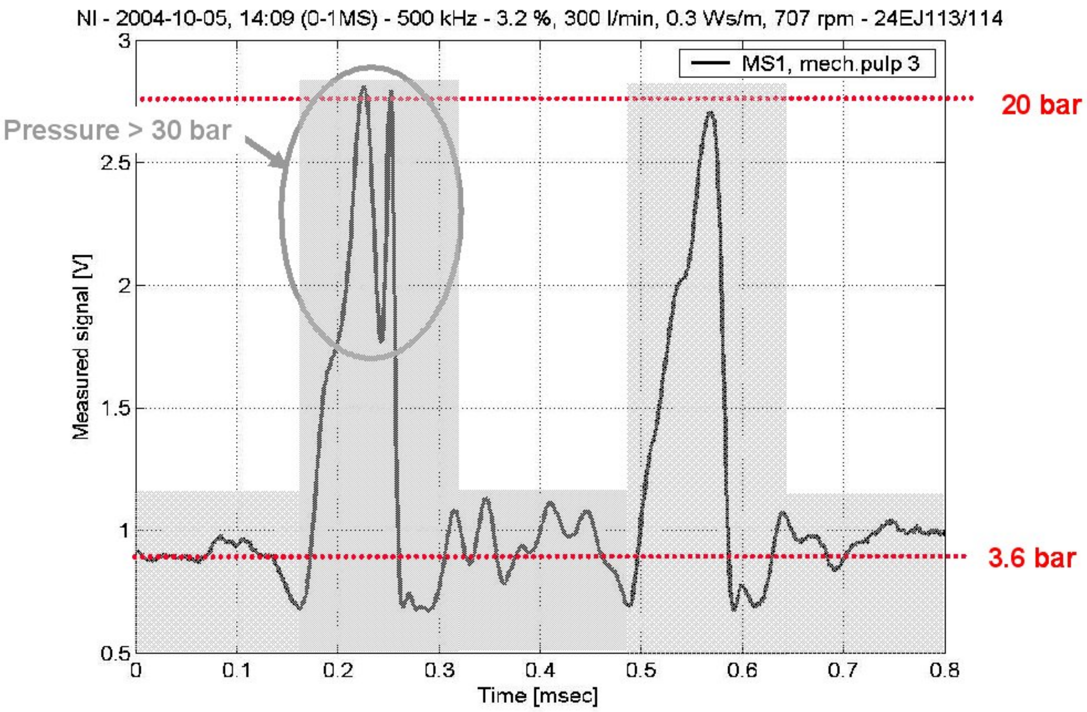

Figure A4: Response from pressure sensor MS1 during refining of a high-freeness TMP. The bar and groove pattern as well as the assumed pressures are superimposed on the raw signal diagram.

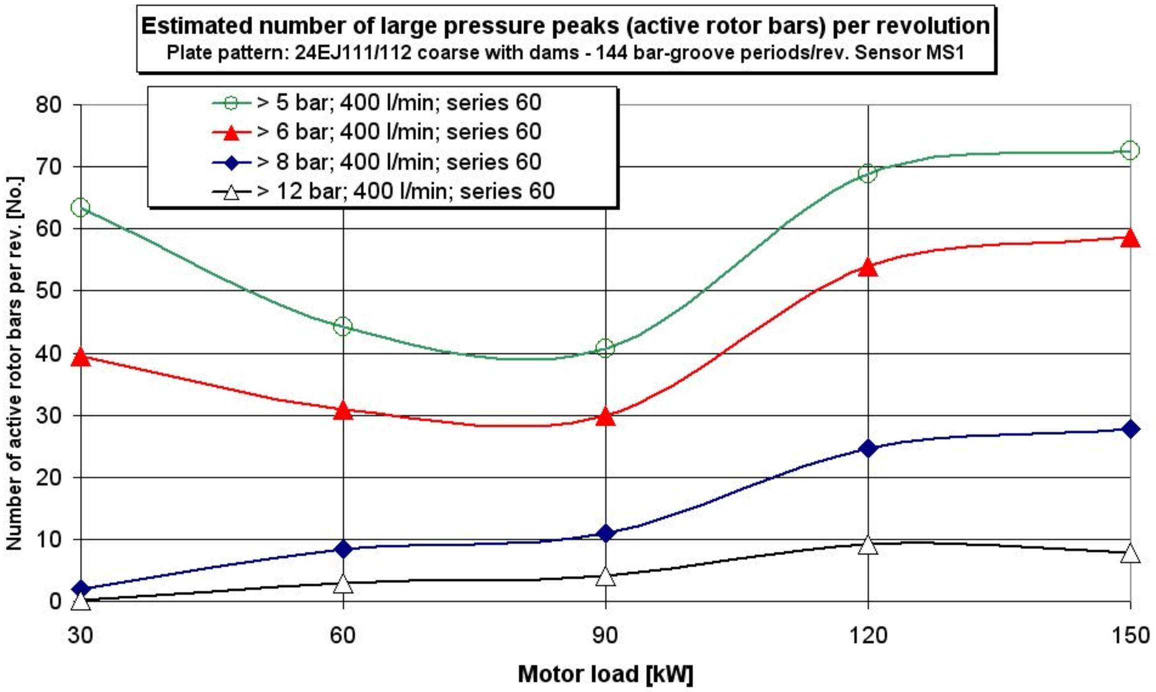

Figure A5: The number of pressure spikes, which are higher than given pressure levels are counted during a refining series of bleached softwood Kraft pulp.

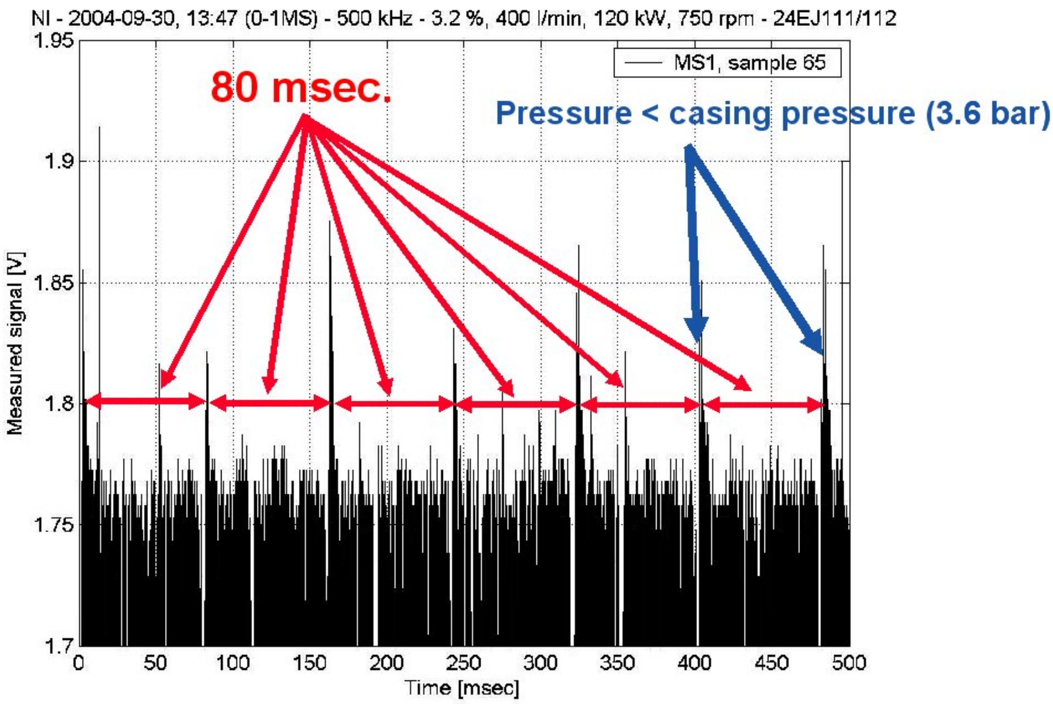

Figure A6: The response from pressure sensor MS1 during refining of bleached softwood Kraft pulp strongly indicates frequently pressure drops below the casing pressure of the refiner. 80 milliseconds between the pressure drops correspond to one event per revolution.

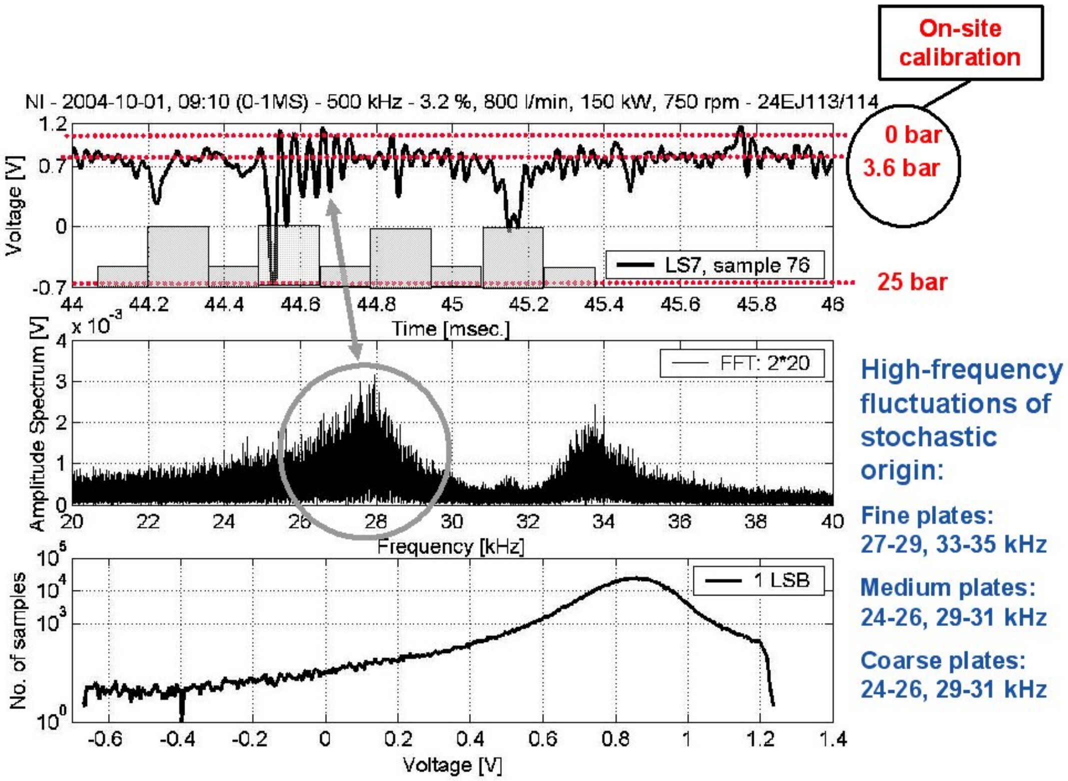

Figure A7: The upper plot shows the response from pressure sensor LS7 during refining of bleached softwood Kraft pulp. It is indicated that the pressure decreases randomly below the atmospheric pressure. In addition some high frequency fluctuations are shown. The latter is revealed through the frequency spectrum in the middle as well. The lower plot shows the histogram of the raw signal. The y-axis is given in log scale.

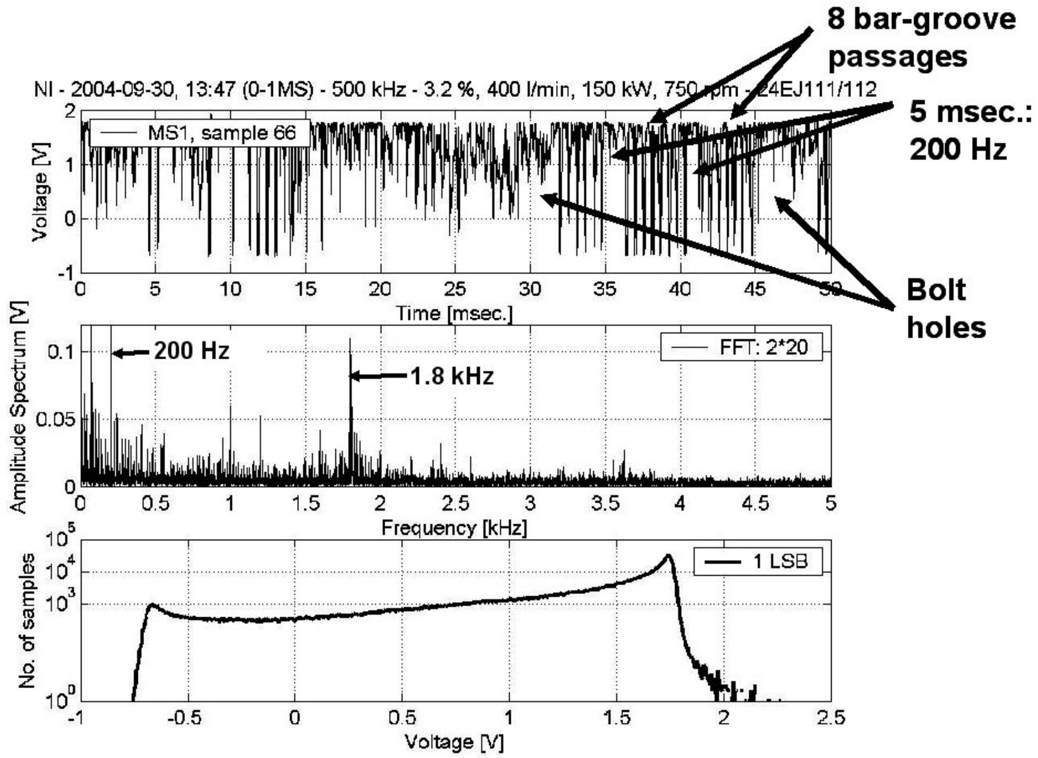

Figure A8: The upper plot shows the response from pressure sensor MS1 during refining of bleached softwood Kraft pulp. Inherent features of the plate pattern are revealed by the number of bars between the bolt holes and flow channels respectively. The number of bars as well as the number of flow channels is revealed through the frequency spectrum in the middle through the frequencies of 1.8 kHz and 200 Hz respectively. The lower plot shows the histogram of the raw signal. The y-axis is given in log scale.

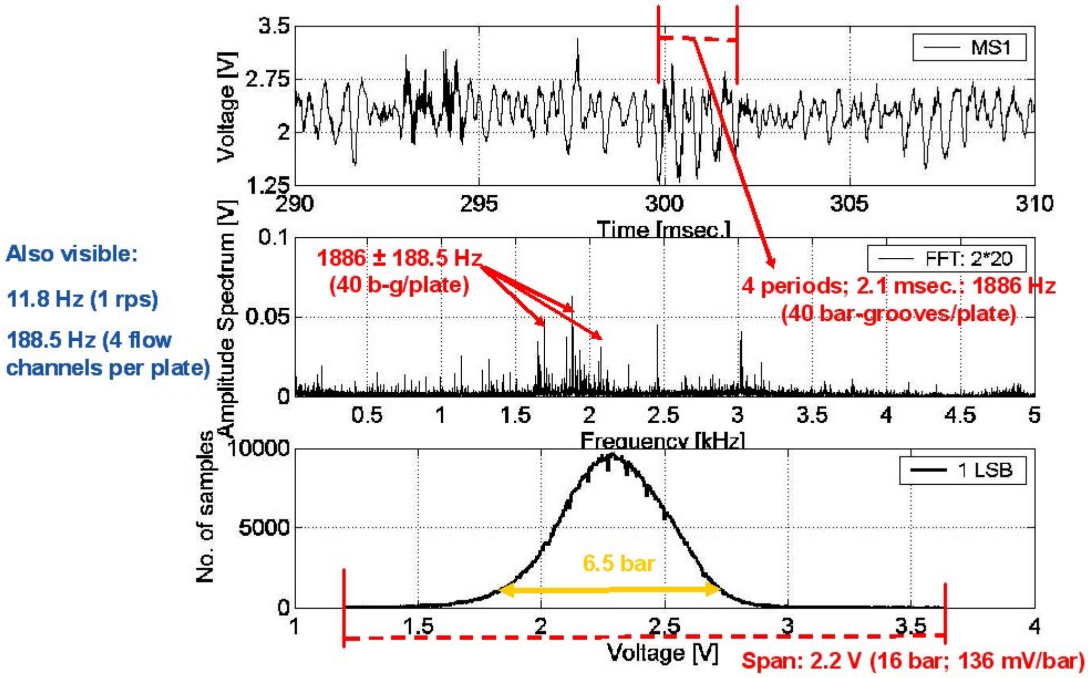

Figure A9: The upper plot shows the response from pressure sensor MS1 during refining of TMP at 700 rpm. Inherent features of the plate pattern are revealed by the number of bars between the bolt holes and flow channels respectively. The number of bars as well as the number of flow channels is revealed through the frequency spectrum in the middle through the frequencies of 1886 and 188.5 Hz respectively. The lower plot shows the histogram of the raw signal.

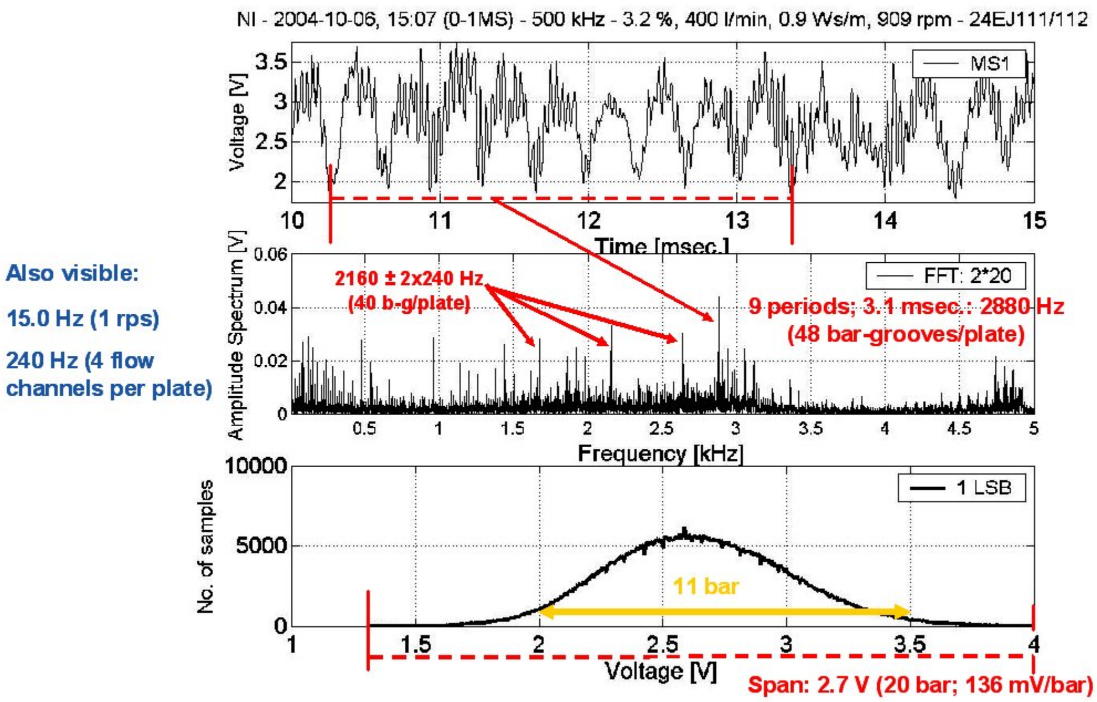

Figure A10: The upper plot shows the response from pressure sensor MS1 during refining of TMP at 900 rpm. Inherent features of the plate pattern are revealed by the number of bars between the bolt holes and flow channels respectively. The number of bars as well as the number of flow channels is revealed through the frequency spectrum in the middle through the frequencies of 2880 and 240 Hz respectively. Sideband frequencies are shown as well. These are given by ±240 Hz about the 2880 Hz frequency. The lower plot shows the histogram of the raw signal.

Appendix B:

Calibration tests in the Material Test System Laboratory (MTS) in connection with the second pressure sensor trial in the spring 2005

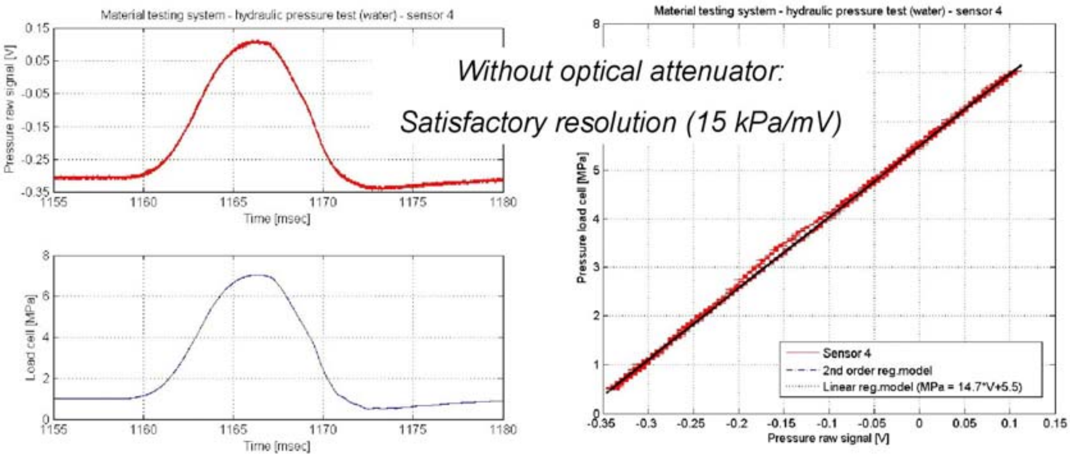

Figure B1: The upper plot on the left hand side shows the pressure response from sensor 4 during impact of a pure hydraulic pressure performed in a water filled chest. The lower plot shows the response from the activating device of the hydraulic pressure. The plot on the right hand side shows a x-y plot of the responses from the activating device and the pressure sensor.

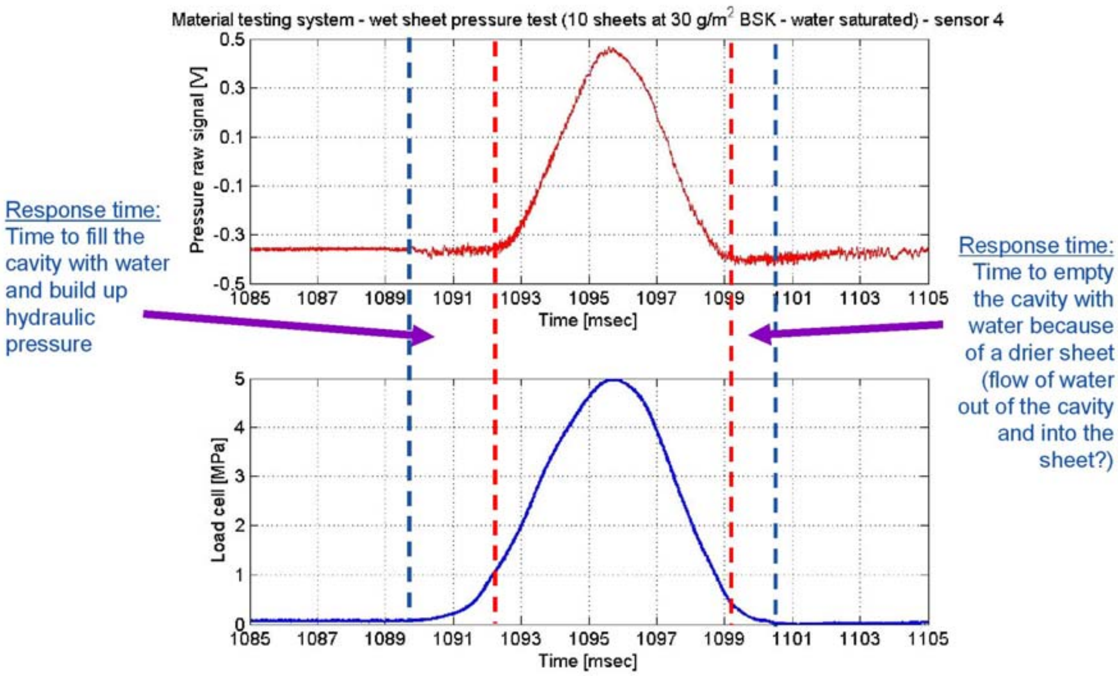

Figure B2: The upper plot shows the raw data from sensor 4 during impact of a load. A layer of 10 water filled sheets was located on the top of the sensor surface.

The lower plot shows the corresponding response from the load cell.

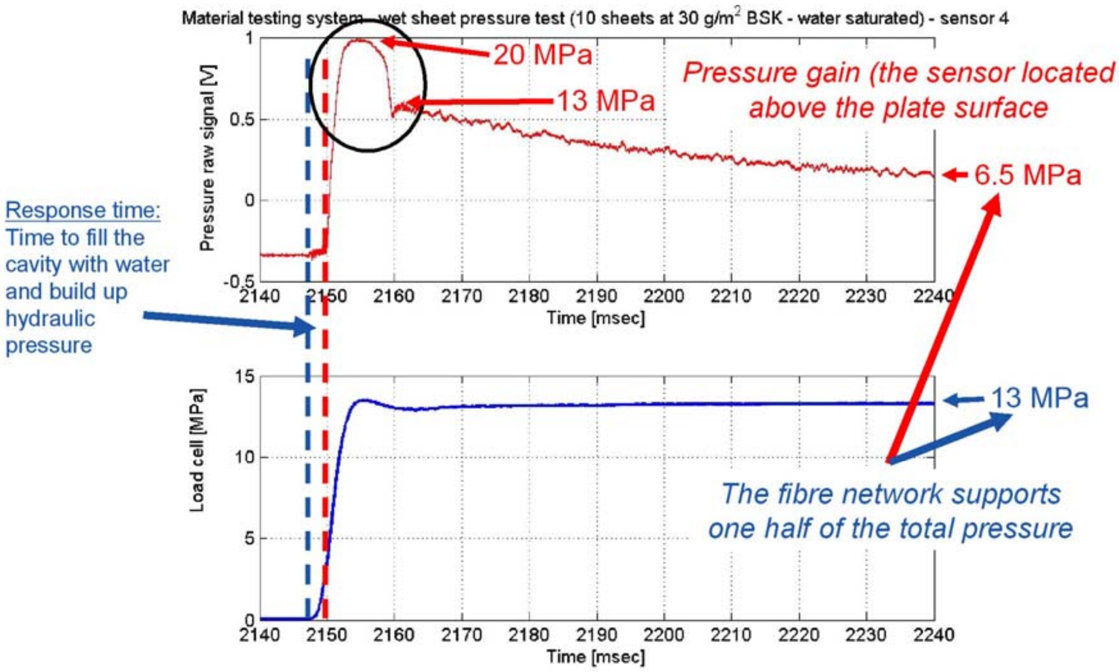

Figure B3: The upper plot shows the raw data from sensor 4 during impact of a load cell performed on a layer of 10 water filled sheets located on the top of the sensor surface. The lower plot shows the corresponding response from the load cell.

Appendix C:

Additional measurement results

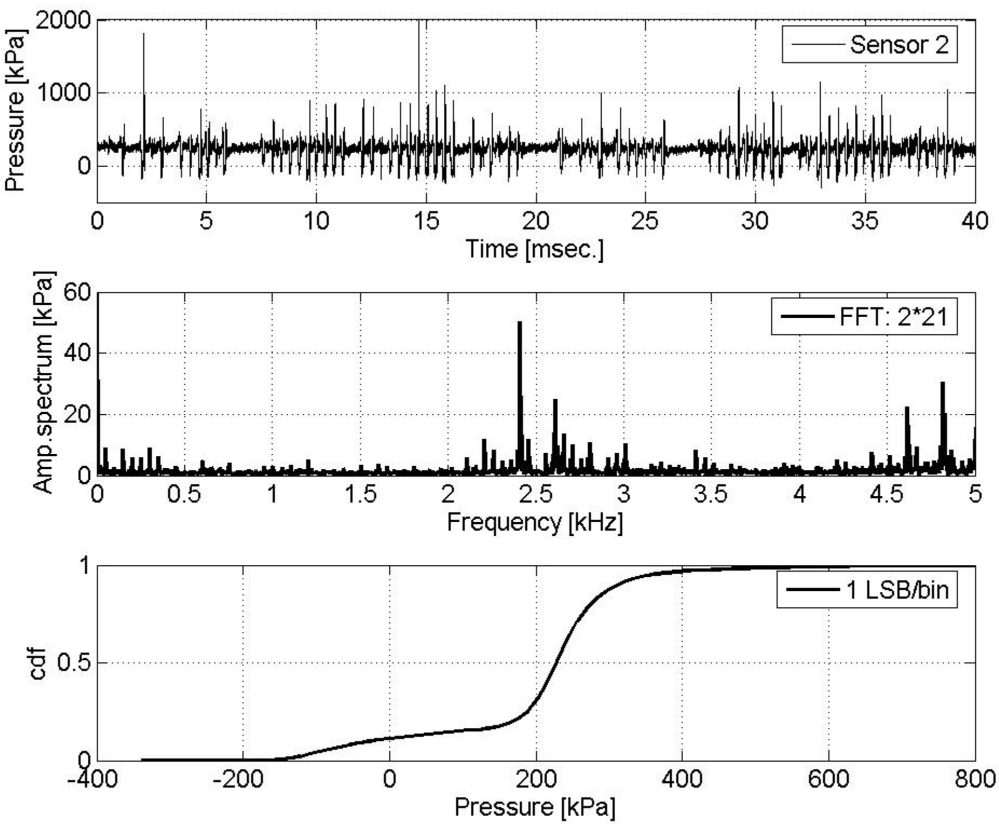

<table>
<tr><th colspan="8">Sample information</th></tr>
<tr><td colspan="3">Sample rate [MS/s]
5</td><td colspan="3">Sample size [MS]
2</td><td colspan="2">LSB [kPa/bit]
13.5</td></tr>
<tr><td colspan="3" rowspan="3">P(average raw) [kPa]
73</td><td colspan="3">P(average adjusted) [kPa]
210</td><td colspan="2" rowspan="3">P(offset) [kPa]
137</td></tr>
<tr><td colspan="3">P(minimum) [kPa]
-338</td></tr>
<tr><td colspan="3">P(maximum) [kPa]
2022</td></tr>
<tr><th colspan="8">Process information</th></tr>
<tr><td colspan="2">Motor load [kW]</td><td colspan="2">Plate gap [µm]</td><td colspan="2">Pressure [kPa]</td><td colspan="2">Temperature [°C]</td></tr>
<tr><td>Gross
220</td><td>Net
150</td><td>Moveable
131</td><td>Fixed
123</td><td>In
209</td><td>Out
396</td><td>In
28.5</td><td>Out
34.9</td></tr>
<tr><td colspan="4">Flow rate [l/min]: 400</td><td colspan="4">Dry solid content [%]: 3.5</td></tr>
</table>

Rotational speed [rpm]: 750	**Rotational direction:** feed

Figure C1: Response from sensor 2 during refining of BSK pulp.

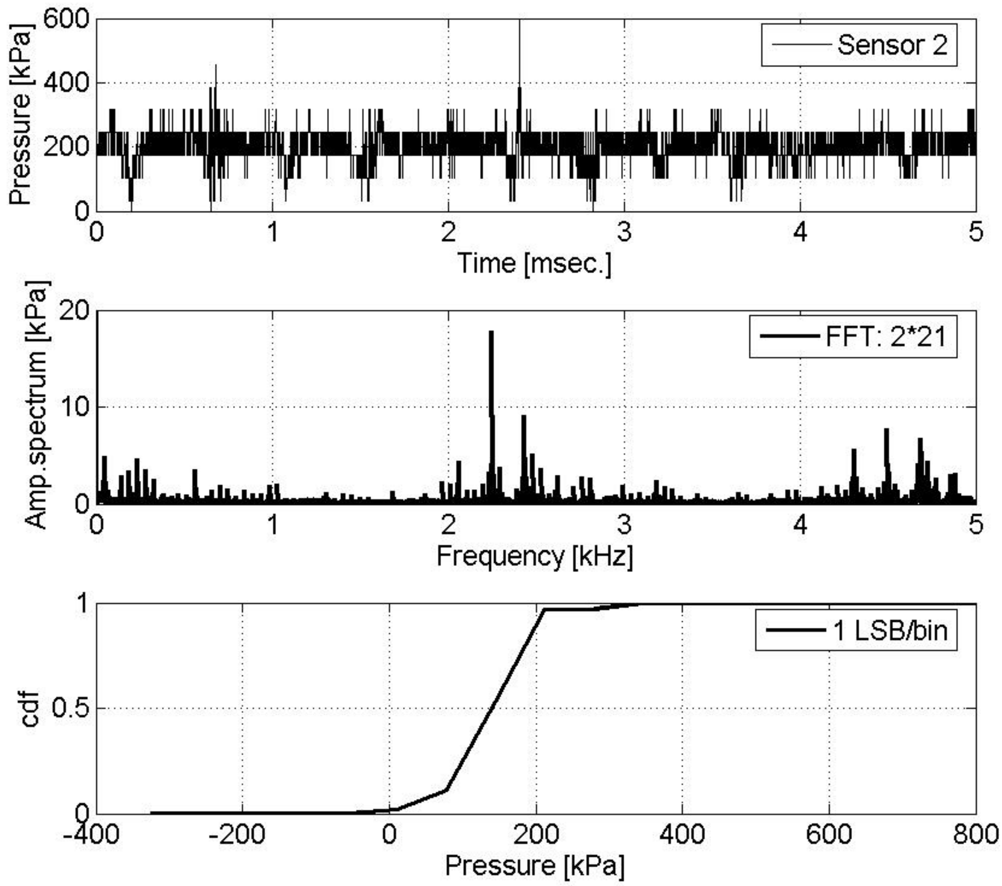

Sample information							
Sample rate [MS/s] 1			**Sample size [MS]** 2		**LSB [kPa/bit]** 67.1		
P(average raw) [kPa] -137			**P(average adjusted) [kPa]** 201		**P(offset) [kPa]** 338		
			P(minimum) [kPa] -325				
			P(maximum) [kPa] 1207				
Process information							
Motor load [kW]		**Plate gap [µm]**		**Pressure [kPa]**		**Temperature [°C]**	
Gross 160	**Net** 88	**Moveable** 60	**Fixed** 198	**In** 201	**Out** 332	**In** 87.0	**Out** 90.0
Flow rate [l/min]: 399				**Dry solid content [%]:** 3.1			
Rotational speed [rpm]: 700				**Rotational direction:** feed			

Figure C2: Response from pressure sensor 2 during refining of high freeness TMP.

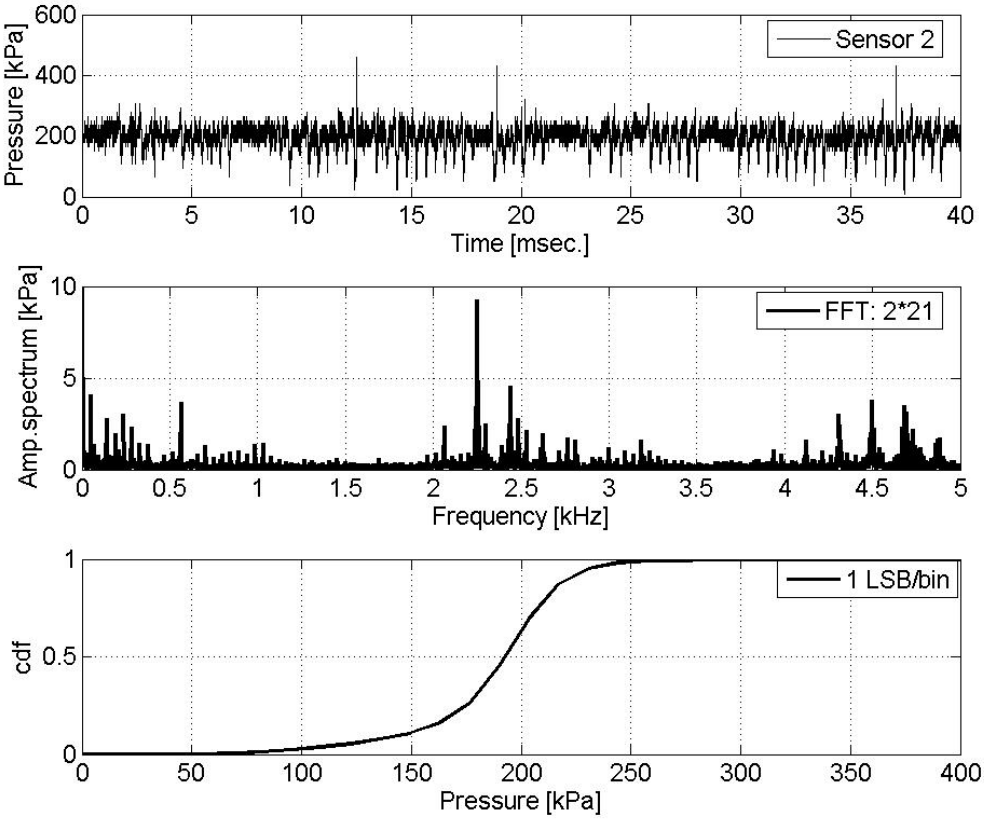

Sample information							
Sample rate [MS/s] 1			**Sample size [MS]** 2			**LSB [kPa/bit]** 13.5	
P(average raw) [kPa] -159			**P(average adjusted) [kPa]** 198			**P(offset) [kPa]** 357	
			P(minimum) [kPa] -162				
			P(maximum) [kPa] 1118				
Process information							
Motor load [kW]		**Plate gap [µm]**		**Pressure [kPa]**		**Temperature [°C]**	
Gross 170	**Net** 93	**Moveable** 108	**Fixed** 239	**In** 198	**Out** 329	**In** 84.2	**Out** 88.0
Flow rate [l/min]: 399				**Dry solid content [%]:** 3.5			
Rotational speed [rpm]: 700				**Rotational direction:** feed			

Figure C3: Response from pressure sensor 2 during refining of high freeness RTS-TMP.

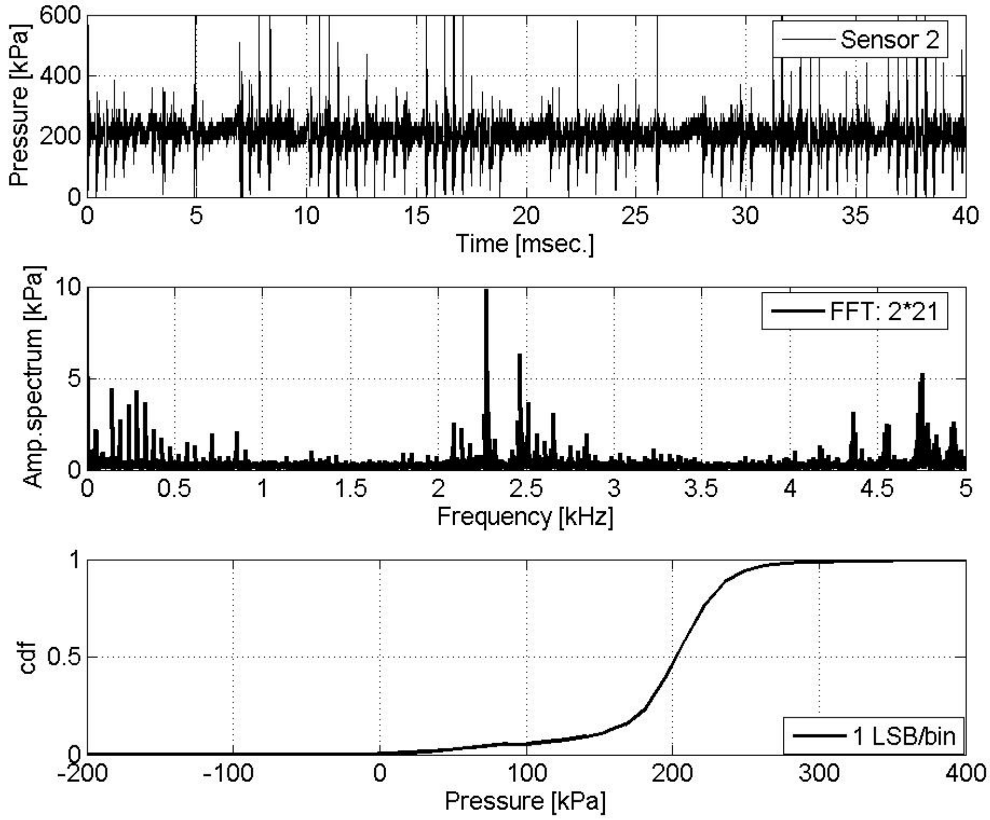

<table>
<tr><th colspan="8">Sample information</th></tr>
<tr><td colspan="3">Sample rate [MS/s]
1</td><td colspan="3">Sample size [MS]
2</td><td colspan="2">LSB [kPa/bit]
13.5</td></tr>
<tr><td colspan="3" rowspan="3">P(average raw) [kPa]
14</td><td colspan="3">P(average adjusted) [kPa]
200</td><td colspan="2" rowspan="3">P(offset) [kPa]
186</td></tr>
<tr><td colspan="3">P(minimum) [kPa]
-333</td></tr>
<tr><td colspan="3">P(maximum) [kPa]
1583</td></tr>
<tr><th colspan="8">Process information</th></tr>
<tr><td colspan="2">Motor load [kW]</td><td colspan="2">Plate gap [µm]</td><td colspan="2">Pressure [kPa]</td><td colspan="2">Temperature [°C]</td></tr>
<tr><td>Gross
153</td><td>Net
88</td><td>Moveable
34</td><td>Fixed
96</td><td>In
200</td><td>Out
262</td><td>In
75.2</td><td>Out
78.4</td></tr>
<tr><td colspan="4">Flow rate [l/min]: 400</td><td colspan="4">Dry solid content [%]: 3.5</td></tr>
<tr><td colspan="4">Rotational speed [rpm]: -700</td><td colspan="4">Rotational direction: expel</td></tr>
</table>

Figure C4: Response from pressure sensor 2 during refining of a blend of high freeness RTS-TMP and one pass low-consistency refined pulp of the same origin.

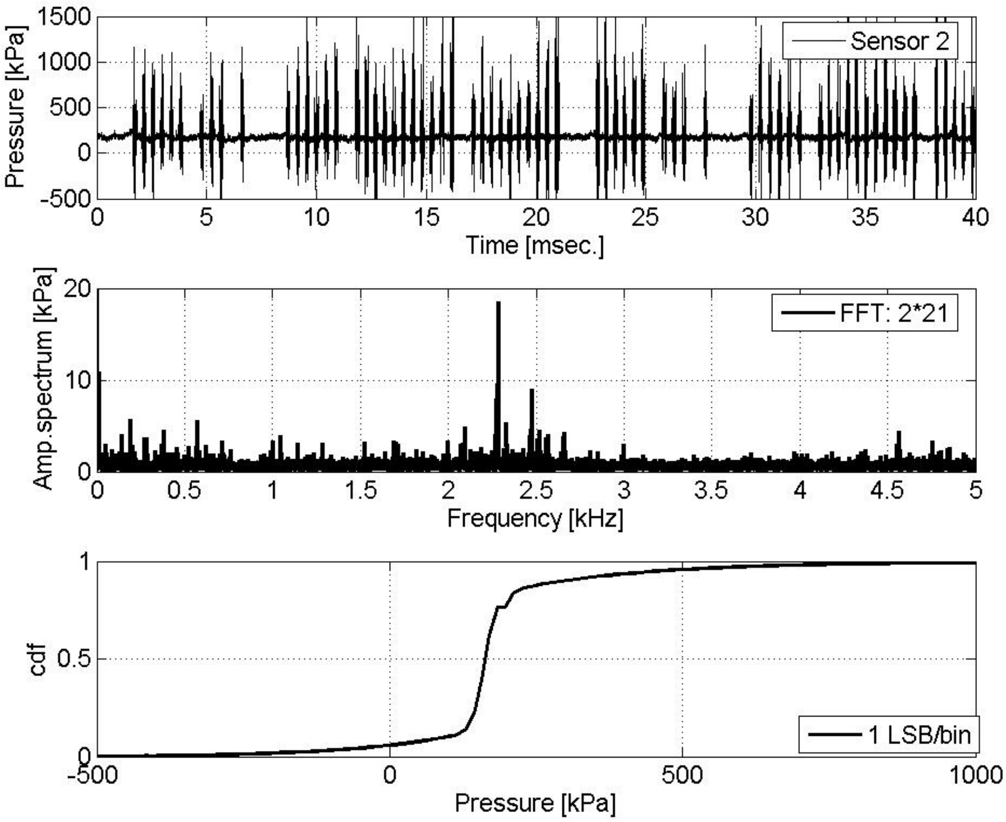

<table>
<tr><th colspan="8">Sample information</th></tr>
<tr><td colspan="3">Sample rate [MS/s]
1</td><td colspan="3">Sample size [MS]
2</td><td colspan="2">LSB [kPa/bit]
13.5</td></tr>
<tr><td colspan="3" rowspan="3">P(average raw) [kPa]
22</td><td colspan="3">P(average adjusted) [kPa]
193</td><td colspan="2" rowspan="3">P(offset) [kPa]
171</td></tr>
<tr><td colspan="3">P(minimum) [kPa]
-709</td></tr>
<tr><td colspan="3">P(maximum) [kPa]
2896</td></tr>
<tr><th colspan="8">Process information</th></tr>
<tr><td colspan="2">Motor load [kW]</td><td colspan="2">Plate gap [µm]</td><td colspan="2">Pressure [kPa]</td><td colspan="2">Temperature [°C]</td></tr>
<tr><td>Gross
62.5</td><td>Net
0</td><td>Moveable
>3000</td><td>Fixed
351</td><td>In
193</td><td>Out
263</td><td>In
23.8</td><td>Out
29.8</td></tr>
<tr><td colspan="4">Flow rate [l/min]: 405</td><td colspan="4">Dry solid content [%]: 0</td></tr>
<tr><td colspan="4">Rotational speed [rpm]: -700</td><td colspan="4">Rotational direction: expel</td></tr>
</table>

Figure C5: Response from pressure sensor 2 when water was pumped through the refiner.

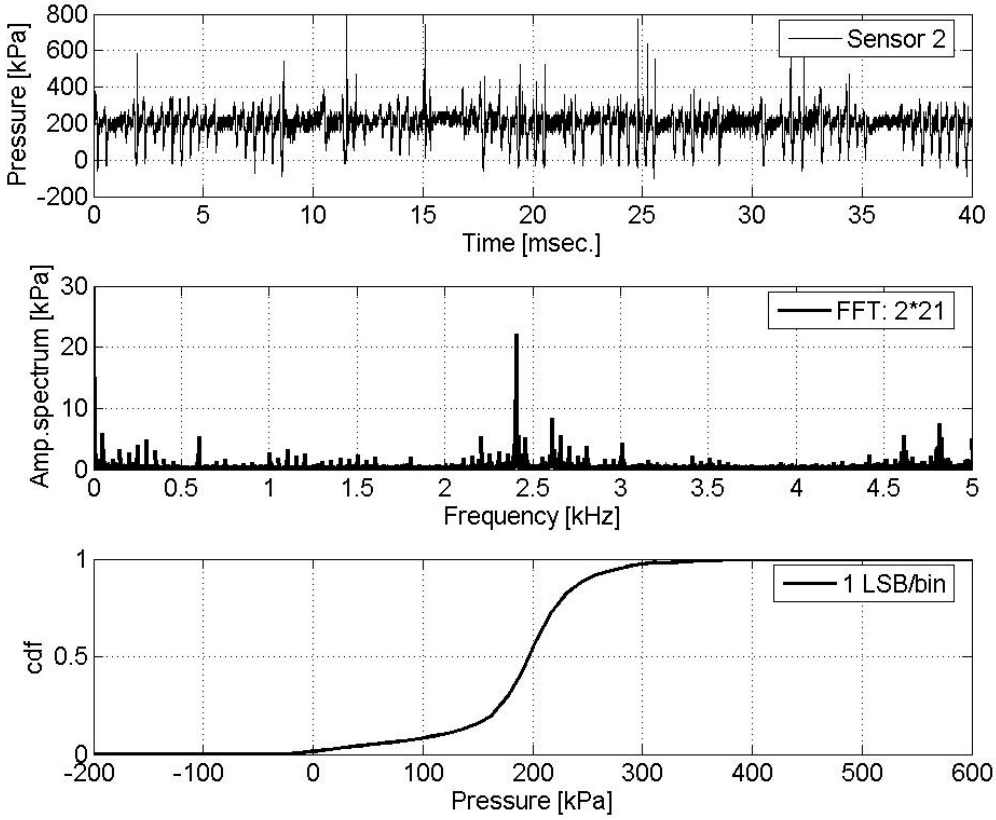

<table>
<tr><th colspan="8">Sample information</th></tr>
<tr><td colspan="3">Sample rate [MS/s]
1</td><td colspan="3">Sample size [MS]
2</td><td colspan="2">LSB [kPa/bit]
13.5</td></tr>
<tr><td colspan="3" rowspan="3">P(average raw) [kPa]
26</td><td colspan="3">P(average adjusted) [kPa]
200</td><td colspan="2" rowspan="3">P(offset) [kPa]
174</td></tr>
<tr><td colspan="3">P(minimum) [kPa]
-202</td></tr>
<tr><td colspan="3">P(maximum) [kPa]
1558</td></tr>
<tr><th colspan="8">Process information</th></tr>
<tr><td colspan="2">Motor load [kW]</td><td colspan="2">Plate gap [µm]</td><td colspan="2">Pressure [kPa]</td><td colspan="2">Temperature [°C]</td></tr>
<tr><td>Gross
223</td><td>Net
146</td><td>Moveable
252</td><td>Fixed
227</td><td>In
199</td><td>Out
368</td><td>In
28.5</td><td>Out
31.1</td></tr>
<tr><td colspan="4">Flow rate [l/min]: 1000</td><td colspan="4">Dry solid content [%]: 4.07</td></tr>
<tr><td colspan="4">Rotational speed [rpm]: 750</td><td colspan="4">Rotational direction: feed</td></tr>
</table>

Figure C6: Response from pressure sensor 2 during refining of bleached softwood kraft pulp.

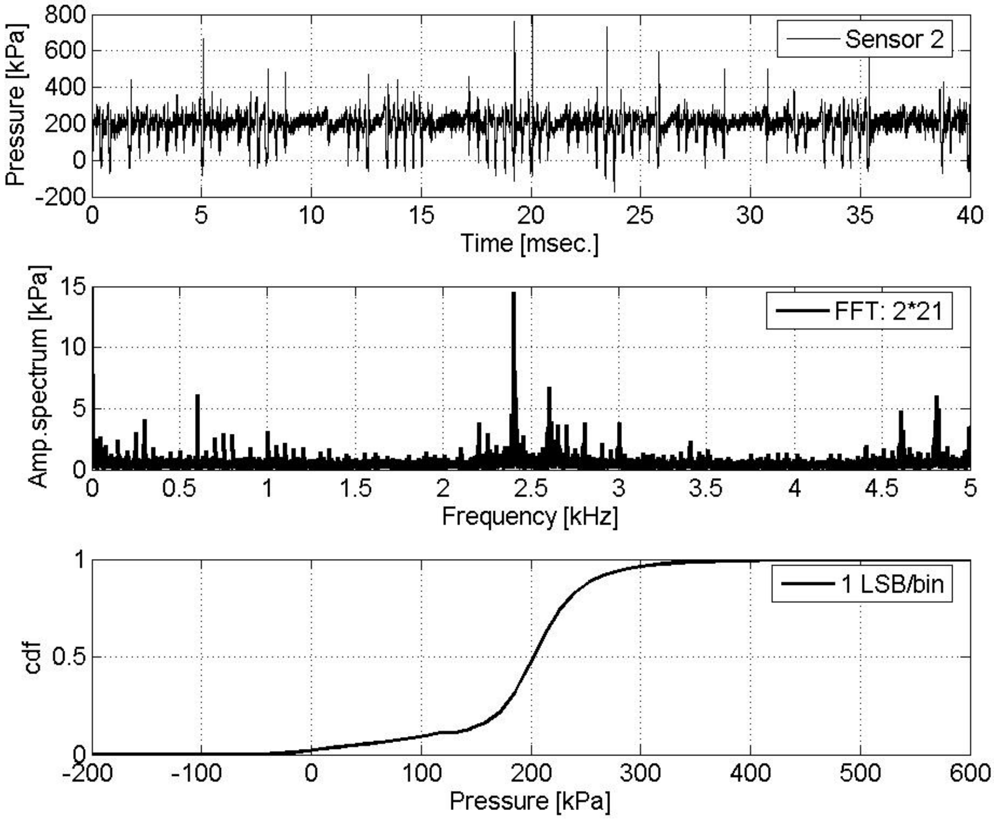

<table>
<tr><td colspan="8">Sample information</td></tr>
<tr><td colspan="3">Sample rate [MS/s]
1</td><td colspan="3">Sample size [MS]
2</td><td colspan="2">LSB [kPa/bit]
13.5</td></tr>
<tr><td colspan="3" rowspan="3">P(average raw) [kPa]
25</td><td colspan="3">P(average adjusted) [kPa]
200</td><td colspan="2" rowspan="3">P(offset) [kPa]
175</td></tr>
<tr><td colspan="3">P(minimum) [kPa]
-315</td></tr>
<tr><td colspan="3">P(maximum) [kPa]
1533</td></tr>
<tr><td colspan="8">Process information</td></tr>
<tr><td colspan="2">Motor load [kW]</td><td colspan="2">Plate gap [µm]</td><td colspan="2">Pressure [kPa]</td><td colspan="2">Temperature [°C]</td></tr>
<tr><td>Gross
226</td><td>Net
154</td><td>Moveable
234</td><td>Fixed
191</td><td>In
202</td><td>Out
366</td><td>In
27.2</td><td>Out
29.9</td></tr>
<tr><td colspan="4">Flow rate [l/min]: 1000</td><td colspan="4">Dry solid content [%]: 2.96</td></tr>
<tr><td colspan="4">Rotational speed [rpm]: 750</td><td colspan="4">Rotational direction: feed</td></tr>
</table>

Figure C7: Response from pressure sensor 2 during refining of bleached softwood

kraft pulp.

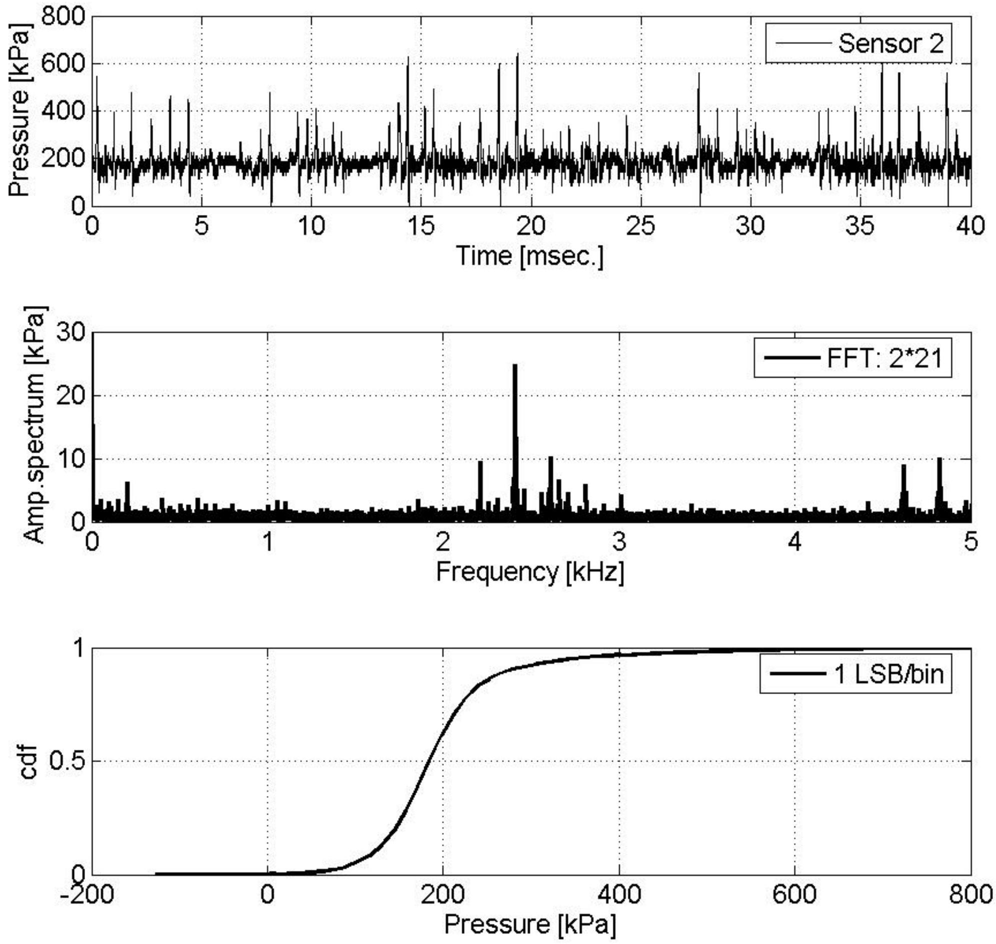

<table>
<tr><th colspan="8">Sample information</th></tr>
<tr><td colspan="2">Sample rate [MS/s]
1</td><td colspan="3">Sample size [MS]
2</td><td colspan="3">LSB [kPa/bit]
13.5</td></tr>
<tr><td colspan="2" rowspan="3">P(average raw) [kPa]
25</td><td colspan="3">P(average adjusted) [kPa]
206</td><td colspan="3" rowspan="3">P(offset) [kPa]
235</td></tr>
<tr><td colspan="3">P(minimum) [kPa]
-127</td></tr>
<tr><td colspan="3">P(maximum) [kPa]
1788</td></tr>
<tr><th colspan="8">Process information</th></tr>
<tr><td colspan="2">Motor load [kW]</td><td colspan="2">Plate gap [µm]</td><td colspan="2">Pressure [kPa]</td><td colspan="2">Temperature [°C]</td></tr>
<tr><td>Gross
181</td><td>Net
109</td><td>Moveable
248</td><td>Fixed
372</td><td>In
206</td><td>Out
361</td><td>In
44.3</td><td>Out
46.6</td></tr>
</table>

Flow rate [l/min]: 902	**Dry solid content [%]:** 3.6
Rotational speed [rpm]: 750	**Rotational direction:** feed

Figure C8: Response from pressure sensor 2 during refining of unbleached softwood kraft pulp.

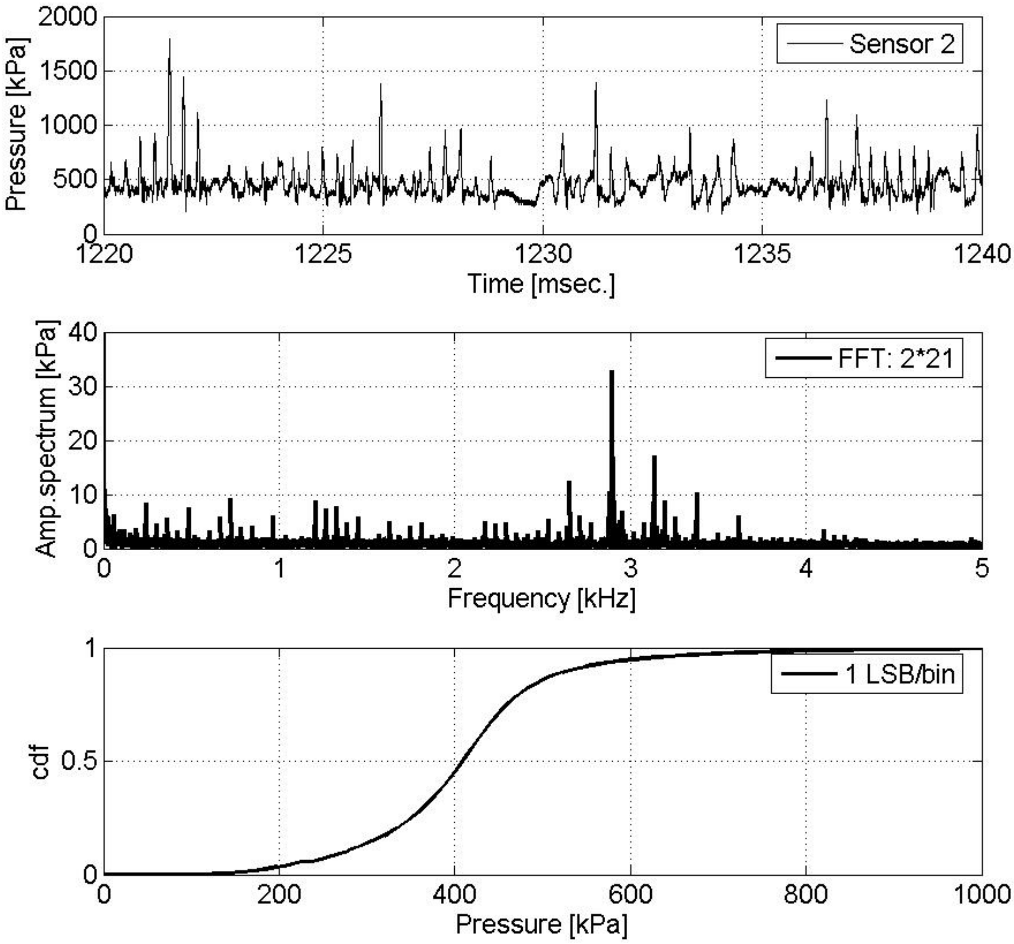

<table>
<tr><th colspan="4">Sample information</th></tr>
<tr><td colspan="2">Sample rate [MS/s]
1</td><td>Sample size [MS]
2</td><td>LSB [kPa/bit]
13.5</td></tr>
<tr><td colspan="2" rowspan="3">P(average raw) [kPa]
25</td><td>P(average adjusted) [kPa]
417</td><td rowspan="3">P(offset) [kPa]
142</td></tr>
<tr><td>P(minimum) [kPa]
-262</td></tr>
<tr><td>P(maximum) [kPa]
2027</td></tr>
<tr><th colspan="4">Process information</th></tr>
<tr><td>Motor load [kW]</td><td>Plate gap [µm]</td><td>Pressure [kPa]</td><td>Temperature [°C]</td></tr>
</table>

Gross	Net	Moveable	Fixed	In	Out	In	Out
257	128	252	495	198	417	41.9	45.2
Flow rate [l/min]: 914 ± 21.5				**Dry solid content [%]:** 3.6			
Rotational speed [rpm]: 900				**Rotational direction:** feed			

Figure C9: Response from pressure sensor 2 during refining of unbleached softwood kraft pulp.

Appendix D:

Theoretical reflections of the conditions in the refining zone

FIBRE QUANTITY AND DENSITY

An attempt to answer the question of how many fibres there are present in the refining zone of a low-consistency refiner is done in this appendix. The conditions in the refining zone are indeed complex. Thus, the derivations deserve a more fundamental approach than given here. No rigorous derivations are used, and the following figures and calculations must be considered as a starting point for further discussions. Some data is collected from scientific works and some data is based on a scientific guess. Hopefully, the simple calculations are reasonable since the equations are derived from simple dimensional analysis of the denominations of the variables.

Table D1: Typical softwood fibre dimensions (Norway spruce *(Picea Abies)*)[1]

	Native	BSK (SR~ 14)	TMP average (CSF~ 100)	TMP long (30-45 %)	TMP medium (30-35 %)	TMP short (25-35 %)
Mean fibre length [mm]	3.2	2.3	1.7	2.0	0.7	0.2
Fibre width [µm]	32	30	25	30		
Coarseness [mg/m]	0.35	0.20	0.25	0.27	0.25	0.25
Fibre wall width [µm]	2.4	3.0	2.2	2.4		
No of fibres (coarseness) [No/g] x 10^6	0.89	2.17	2.35	1.85	5.7	20.0
No of fibres (wall density) [No/g] x 10^6	1.76	2.12	2.47	1.88		

[1] Sources: Braaten (1996), Kure (1999), Mörseburg (2004), Solheim (2005)

Table D1 shows typical data of some fibre dimensions from Norway spruce. The number of fibres per gram is derived from two approaches given by the coarseness and the fibre wall density respectively. Figure D1 shows an illustration of the fibre dimensions. Intuitively, the two approaches should provide the same number. The table reveals some minor differences, which in turn signifies that some of the basic figures of the variables are not accurately determined.

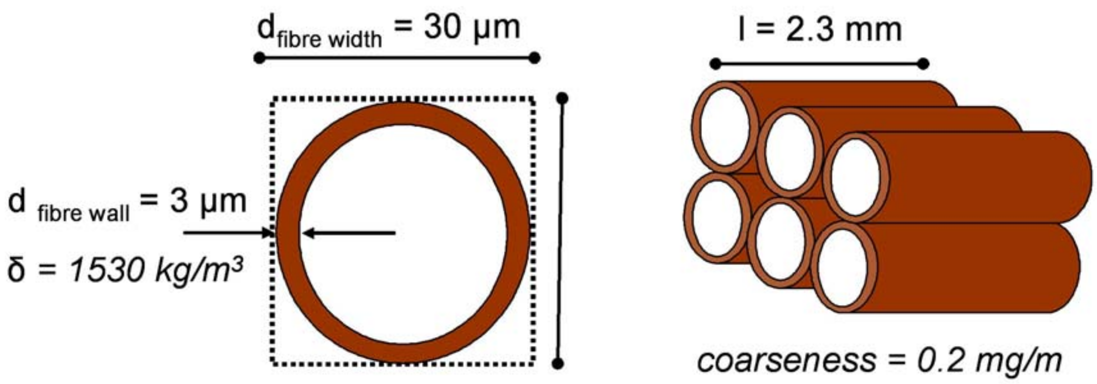

Figure D1: Fibre dimensions.

The following number of fibres in a definite volume and the corresponding density are derived from an approach with certain limitations. These limitations assume that only intact fibres (no collapse is assumed) are present, and that the fibres are aligned such that an outer extension volume (square) of the fibres occupies the volume.

No of fibres per litre: 483 000 000

Density: 220 kg/m^3

REFINER DATA

Table D2 shows typical numbers of the refiner plates and the disc size of the Beloit DD refiner at STFI-Packforsk EuroFEX laboratory.

Table D2: Typical refiner disc and refiner plate dimensions (Beloit DD 600 mm)

Plate pattern		Refiner disc	
Bar width [mm]	3.0	Inlet radius [m]	0.19
Groove width [mm]	4.4	Outlet radius [m]	0.30
Bar height [mm]	7.3	Plate area [m^2]	0.17
Bar area [m^2]	0.07	Bar area fract. [%]	41
Bar intersection area [m^2]	0.03	Bar intersection area fraction [%]	16

The consistency of the pulp suspension at typical running conditions is 35 g/l. The corresponding number of fibres per litre assuming a quantity of 2.2 million fibres per gram is 77 million (77 000 000 fibres/litre).

Table D3 shows calculated number of fibres in the refining zone.

Table D3: Theoretical derived the number of fibres in the refining zone

Plate gap [µm]	300	200	100
Refining zone volume [litre]	1.52	1.50	1.49
Bar intersection volume [litre]	0.008	0.006	0.003
No of fibres in the refining zone (35 g/l) [No] x 10^6	117	116	114
No of fibres in the bar intersection (35 g/l) [No] x 10^6	0.64	0.43	0.21
No of fibres in the bar intersection (220 kg/m^3) [No] x 10^6	4.0	2.7	1.3
Fraction of fibres in the bar intersection area assuming a high fibre concentration (220 kg/m^3) in the plate gap compared to the overall consistency (35 g/l) [%]	3.4	2.3	1.1
Mass concentration in the bar intersection area [mg/cm^2]	6.7	4.4	2.2
Mass concentration (experimental data)[2] [mg/cm^2]	~9	~6	~3

2

PRESSURE DROPS AND FLOW MECHANISMS

According to Duffy et al. 2003 and 2005, the flow mechanisms (friction loss) of fibre suspensions (< 1.9 % consistency) in small diameter pipes (> 3.77 mm) correspond to the water flow behaviour. This has been experimental observed at flow velocities smaller than 3 m/s. If a bar to bar passage assumes to be a channel (pipe), the flow mechanisms should be similar in the bar intersection areas of the refiner. However, the conditions in the refiner are different compared to the conditions in the pipes

---

[2] Source: May et al. (1988) – experimental data from a laboratory press device during impact of load on high-consistency mechanical pulp.

investigated by Duffy and co-workers. The consistency is in the order of 3-4 %, while the tangential flow in the plate gap may approach 15-20 m/s, which is the speed of the rotor disc at a rotational speed in the order of 700-900 rpm.

Assuming a pressure drop during a bar to bar passage (3.0 mm) of 500 kPa, the corresponding pipe friction loss in the plate gap is determined. Figure D2 shows the calculated value (166 000 kPa/m) together with data from Duffy et al. 2005.

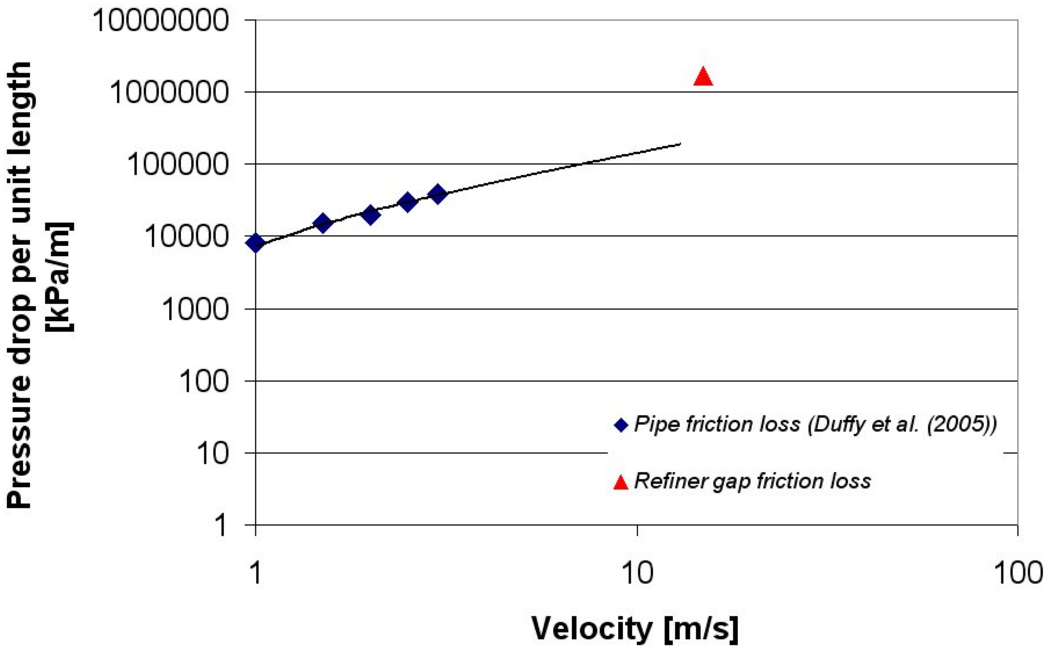

Figure D2: Friction loss data.

The flow mechanisms in the plate gap are probably laminar because the gap is narrow of some 100-300 µm. The corresponding Reynolds number is evidently smaller than the number associated with the transition phase between laminar and turbulent flow, which is assumed to be approximately 2000. The following Reynolds number is derived from two clearly different coefficients of viscosity:

Reynolds number (coefficient of viscosity: 1 Pa.s) : < 1
Reynolds number (coefficient of viscosity: 1 mPa.s (water)) : < 150

The yield stress of a pulp suspension is assumed to be in the order of 0.1-1 kPa (Wikström and Rasmuson (1998), Wikström et al. (2002)). This signifies that the transition from laminar to turbulent flow occurs at a shear stress corresponding to the yield stress. The calculated shear stress of the pulp suspension in the plate gap is shown next. Two different approaches are used. These are reported by Barnes et al. 1989 and Norman et al. 1977 respectively.

Shear stress: $\tau = \frac{\eta \cdot U}{d} [Pa]$ → 100 kPa (U=15 m/s, d= 150 µm, η = 1 Pa.s); 0.1 kPa (U=15 m/s, d= 150 µm, η = 1 mPa.s)

Shear stress: $\tau = \frac{\Delta P}{L} \cdot \frac{r}{2} [Pa]$ = 6.3 kPa (ΔP=500 kPa, L= 3 mm, r = 75 µm)

The upper equation derives the shear stress as a function of the coefficient of viscosity, while the lower equation derives the shear stress from the friction loss. A high coefficient of viscosity signifies that the pulp suspension is in a turbulent phase in the plate gap. Assuming a coefficient of viscosity of water the shear stress is probably below the yield stress and the corresponding flow is probably laminar. The shear stress derived from the friction loss approaches the assumed level of yield stress. It is far from enough data to make any conclusion at all. There are clearly uncertainties associated with the different variables. However, the calculations may be a starting point for further discussion about the flow mechanisms and the viscosity properties of the pulp suspension in the small plate gap in the refiner.

REFERENCES

Barnes, H.A., Hutton, J.F. and Walters, K. (1989): *"An introduction to rheology."* Elsevier Science B.V, Amsterdam, The Netherlands, 199 p., ISBN: 0-444-87469-0.

Braaten, K.R. (1996): *"The impact of site and wood properties on thermo mechanical pulp. Classification of wood for more uniform TMP-quality."* Doctoral thesis, Department of Forest Sciences, Agricultural University of Norway, 27, 137 p., ISBN: 82-575-0297-9.

Duffy, G.G. and Ramachandra, S. (2005): *"Validation of flow mechanisms of fibre suspensions in small diameter pipes"* Appita., 58 (5), pp. 374-377.

Duffy, G.G. and Abdullah, L. (2003): *"The flow of fibre suspensions in small diameter pipes"* Appita., 56 (4), pp. 290.

Kure, K.A. (1999): *"On the relationship between process input variables and fibre characteristics in termomechanical pulping."* Doctoral thesis, Department of Chemical Engineering, Norwegian University of Science and Technology, 45, 123 p., ISBN: 82-471-0412-1.

May, W.D., McRae, M.R., Miles, K.B. and Lunan, W.E. (1988): *"An approach to the measurement of pulp residence time in a chip refiner."* J. Pulp Pap. Sci., 14 (3), pp. J47-J53.

Mörseburg, K. (2004): Confidential report, PFI.

Norman, B., Moller, K., Ek, R. and Duffy, G.G.: "Hydrodynamics of papermaking fibres in water suspension." Trans. "Fibre-water interactions in paper-making", Symposium, Oxford, UK. 1, pp. 195-249, (1977).

Solheim, O. (2005): *"Properties of Norway spruce"* Project report SSFF prosjekt – Norsk trevirke som råstoff. Verdiskapningspotensial og industrielle muligheter, PFI, 17 p.

Wikström, T., Rönnemark, Y. and Rasmuson, A. (2002): *"A new correlation for the onset of fluidisation in pulp suspensions."* Nordic Pulp Pap. Res. J. 17 (4), pp. 374-381.

Wikström, T. and Rasmuson, A. (1998): *"Yield stress of pulp suspensions. The influence of fibre properties and processing conditions"* Nordic Pulp Pap. Res. J. 13 (3), pp. 243-250.